Title

Regulation of Somatic Cell Fate by Escargot in Drosophila Testis

Author

Kryza, Jordan Ryan

Publication Date

2024

Peer reviewed|Thesis/dissertation

UNIVERSITY OF CALIFORNIA

Los Angeles

Regulation of Somatic Cell Fate by Escargot in *Drosophila* Testis

A dissertation submitted in partial satisfaction of the

requirements for the degree Doctor of Philosophy

in Molecular Biology

by

Jordan Ryan Kryza

2024

ABSTRACT OF THE DISSERTATION

Regulation of Somatic Cell Fate by Escargot in *Drosophila* Testis

by

Jordan Ryan Kryza

Doctor of Philosophy in Molecular Biology

University of California, Los Angeles, 2024

Professor Jeffrey Aaron Long, Chair

Adult stem cells are crucial for tissue homeostasis and repair. Their fate is tightly regulated by intrinsic genetic factors and extrinsic cues within the stem cell niche. These niches are adaptable, responding to stimuli to maintain homeostasis, but the molecular details of this regulation are not fully understood. This study explores a mechanism that regulates the fate of somatic support cells in the *Drosophila* testis to maintain tissue homeostasis.

The hub in the *Drosophila* testis niche secretes factors that regulate germline stem cells (GSCs) and cyst stem cells (CySCs). Our lab previously reported that the Snail family transcriptional regulator Escargot (Esg) is necessary for maintaining the identity of both CySCs and hub cells. Depleting *esg* from hub cells leads to their conversion into CySCs, resulting in the loss of both

GSC and CySC populations. Similarly, *esg* depletion from early somatic cells causes CySCs to differentiate prematurely into daughter cyst cells. These findings indicate that Esg is central to determining somatic cell fates, although the mechanisms are not fully understood.

In the adult testis, Egfr activity is low in hub cells under homeostatic conditions but active in CySCs and early cyst cells, regulating their differentiation. Interestingly, Esg protein levels are significantly higher in hub cells than in cyst cells. We hypothesized that Esg influences somatic cell fate by repressing the Egfr signaling cascade. Our results show that repressing Egfr signaling suppresses hub-to-CySC conversion upon *esg* depletion. Conversely, overexpressing *esg* in CySCs increases the number of early cyst cells and induces CySC-to-hub cell conversion, which depends on Egfr activity. Constitutive Egfr activation in CySCs prevents this conversion upon *esg* overexpression. These findings support the hypothesis that Escargot acts upstream of Egfr to regulate somatic cell identity and maintain tissue homeostasis in the testis.

The dissertation of Jordan Ryan Kryza has been approved.

D. Leanne Jones

Amander Therese Clark

Todd Nystul

David William Walker

Jeffrey Aaron Long, Chair

University of California, Los Angeles

2024

Table of Contents

List of Figures

Acknowledgments

I extend my deepest gratitude to Leanne for her unwavering support and guidance throughout this project. My heartfelt thanks also go to Rafael, whose insights have significantly advanced the progress of this work. Both have provided invaluable feedback, and their wisdom has been instrumental in shaping my approach to scientific challenges. My time in Leanne's lab has greatly refined my abilities as a scientist and amplified my enthusiasm for the craft.

Chapter 2 is adapted from a manuscript in preparation.

Kryza J, Sênos Demarco R, Mollenauer R., D'Alterio C, Southall TD, Brand AH, and Jones DL. (2024). Escargot controls somatic cell fate by attenuating EGFR signaling. *In preparation.*

RSD designed and performed experiments and data analysis relating to CySC-to-hub conversion. RM performed lineage tracing experiments for larval studies, aging studies, and Ras effector loop mutations. CD performed experiments pertaining to *esg* transcript localization in the testis. TDS and AHB were involved in generating DamID tracks for Egfr. All other experiments were performed by JRK. DLJ, RSD, and JRK were involved in the design of all experiments and interpretation of results

This work was supported by the National Institute of Health, the UCLA BSCRC Training Program/Rose Hills Foundation for Science & Engineering, and the UCLA Cellular and Molecular Biology T32 training program.

Vita

Education

University of California Los Angeles, Los Angeles, CA — July 2017 – June 2024
Ph.D. Candidate, Molecular Biology

University of Illinois at Urbana-Champaign, Urbana, IL — Aug. 2012 – May 2017
B.S., Molecular and Cellular Biology
High Distinction

Experience

Univ. of California Los Angeles, MCDB Dept. — Apr. 2020 – June 2020
Teaching Assistant — Jan. 2019 – Mar. 2019
MCDB 144, Molecular Biology of Cellular Processes

Leanne Jones Laboratory: Stem cell behavior and dynamics *in vivo* — Jan. 2017 – Present
Graduate Student Researcher
Mechanisms of Stem Cell Niche Maintenance and Regeneration

Steven Blanke Laboratory: Molecular mechanisms of pathogenesis and infectious disease — Sept. 2014 – May 2017
Undergraduate Researcher
Novel mechanisms of modulating host-cell autophagy by pathogen-induced genotoxic stress

Brian Diers Laboratory: Soybean breeding and genetics — May 2014 – Aug. 2014
Laboratory Assistant

Research Fellowships and Awards

UCLA BSCRC Training Program: Rose Hills Foundation Science & Engineering Graduate Scholarship	2019, 2020
UCLA Cellular and Mol. Bio T32 Training Program (NIH T32, PI-Torres)	2018
Harvey L. Pretula Memorial Award for Undergraduate Research Achievement in Microbiology	2017
Alice Helm Award for Undergraduate Research in Microbiology	2016
Francis M. and Harlie M. Clark Undergraduate Research Award	2015

Publications

Kryza J, Sênos Demarco R, Mollenauer R., D'Alterio C, Southall TD, Brand AH, and Jones DL. (2024). Escargot controls somatic cell fate by attenuating EGFR signaling. *Manuscript in Preparation.*

Lieu, D. J., Crowder, M. K., **Kryza, J**. R., Tamilselvam, B., Kaminski, P. J., Kim, I.-J., Li, Y., Jeong, E., Enkhbaatar, M., Chen, H., Son, S. B., Mok, H., Bradley, K. A., Phillips, H., & Blanke, S. R. (2024). Autophagy suppression in DNA damaged cells occurs through a newly identified p53-proteasome-LC3 axis. *BioRxiv*, 2024.05.21.595139.

Presentations

Kryza J, Sênos Demarco R, Mollenauer R, and Jones DL. (2023, March 1-5). Escargot controls somatic cell fate by attenuating EGFR signaling. Poster. 64th Annual *Drosophila* Research Conference, Chicago, IL

Kryza J, Sênos Demarco R, Mollenauer R, and Jones DL. (2022, Oct. 28-29). Escargot modulates Egfr activity to control somatic cell fate in *Drosophila* testis. Poster. USCF Developmental and Stem Cell Biology Program Retreat, Santa Cruz, CA

Kryza J., Voog J., & Jones D. L. (2019) The Role of Escargot in Stem Cell Niche Maintenance in the *Drosophila* Testis. Poster presented at: UCLA Molecular, Cellular, and Developmental Biology Research Conference. Santa Barbara, CA, Dec. 6- Dec. 8, 2019; UCLA MBIDP Recruitment Events. Los Angeles, CA. Jan. 17 & Feb 7, 2020;16th Annual Stem Cell Symposium. Los Angeles, CA, Feb 7, 2020

Kryza J., Sandall, S., Voog, J., Jones, D.L. The Role of Escargot in Stem Cell Niche Maintenance in the *Drosophila* Male Germline. Poster presented at: 2019 MBIDP Recruitment Event. Los Angeles, CA, Feb. 8, 2019;

Kryza J., Sandall, S., Voog, J., Jones, D.L. The Role of Escargot in Stem Cell Niche Maintenance in the *Drosophila* Male Germline. 2018 MCDB Departmental Retreat. Lake Arrowhead, CA, Dec. 1-3, 2018

Lieu D. J., **Kryza J.**, Tamilselvam B., Jeong E., Kaminski P., Schaefer Z. P., Chen H., Mok H., Son S., Phillips H., Blanke S. R. Genotoxic Activity of Pathogenic Bacteria Short-Circuits Host Autophagy. Poster presented at: 2017 ASM Microbe. New Orleans, LA, June 1-5, 2017.

Kryza J., Lieu D. J., Jeong E., Kaminski P., & Blanke S. R. (2017) Bacterial Genotoxin Induced DNA Damage Response Impairs Host-Cell Stress Responses. Poster presented at: 2017 Undergraduate Research Symposium. Urbana, IL, April 23, 2017.

Kryza J., Lieu D. J., Jeong E., Kaminski P., & Blanke S. R. (2016) Genotoxin activity modulates cellular autophagy via the DNA damage response. Poster presented at: 2016 Midwest Microbial Pathogenesis Conference. Urbana, IL, September 23-25, 2016.

Lieu D. J., **Kryza J**., Schaefer Z.P., Tamilselvam B., Mok H., Chen H., Philips H., & Blanke S. R. (2016) Subversion of Host Cell Autophagy by Genotoxic Pathogenic Bacteria. Poster presented at: 2016 ASM Microbe. Boston, MA, June 16-20, 2016.

Lieu, D. J., **Kryza, J.,** Mok, H., Phillips, H., & Blanke, S. R. (2016) Ex-Vivo/In-vivo Models for the Study of Host Responses to Bacterial Genotoxins. Poster presented at: University of Illinois College of Veterinary Medicine Research Day. Urbana, IL, April 20, 2016.

Kryza J., Lieu D. J., & Blanke S. R. (2016) Bacterial Genotoxin Induced DNA Damage Response Modulates Autophagy. Poster presented at: 2016 Undergraduate Research Symposium, Urbana, IL, April 21, 2016.

Lieu D. J., Tamilselvam B., Chen H., **Kryza J.**, Mok H., & Blanke S. R. (2015) Cellular Stress Responses Converge during Intoxication with a Bacterial Genotoxin. Poster presented at: 2015 Microbiology Research Conference. Champaign, IL, October 15, 2015.

Chapter 1: Escargot and Its Role in the *Drosophila* Testis Stem Cell Niche

Introduction

Adult stem cells are essential for tissue homeostasis and repair. With their unique ability to self-renew, stem cells can provide a consistent supply of specialized cells required for organ function and regeneration. Stem cell fate is tightly regulated by many intrinsic, genetic factors and extrinsic cues that are present in the stem cell niche. Stem cell niches are labile; the interdependent cell populations that comprise the niche respond to stimuli to maintain homeostasis, but the molecular details on how this is achieved are incomplete.

For this work, we used the *Drosophila* testis stem cell niche as a model to investigate cell fate decisions. This system is excellent for studying stem cell behavior and niche biology because of the extensive molecular and genetic tools available for cell-specific manipulation of conserved signaling pathways *in vivo*. Research using *Drosophila* has significantly advanced our comprehension of developmental biology, with many findings directly enhancing our understanding of human development and disease. *Drosophila* remains a genetic workhorse model and a vital research tool for studying the molecular networks that are top candidates for regenerative medicine therapeutics.

Overview of the *Drosophila* testis stem cell niche

At the tip of the testis, germline stem cells (GSCs) and somatic cyst stem cells (CySCs) surround a cluster of quiescent somatic cells known as hub cells (Figure 1A). These three cell types work in concert to ensure the proper function and maintenance of the stem cell niche. Hub cells serve as a physical anchor for both GSCs and CySCs, ensuring their proper positioning and adherence within the niche. Additionally, hub cells regulate the behavior and maintenance of both stem cell populations by secreting signaling factors such as Unpaired (Upd) and Decapentaplegic

(Dpp). Germline stem cells divide to self-renewal and to generate a daughter gonialblast (GB), which undergoes four rounds of transit-amplifying (TA) mitotic divisions before initiating spermatocyte-specific gene expression. Subsequently, spermatocytes progress through meiosis to produce haploid spermatids, ultimately maturing into sperm. In parallel, cyst stem cells divide to produce cyst cells (CCs), which can either give rise to a new CySC or, in conjunction with another CC, encapsulate the GB and embark on differentiation alongside the developing germline cyst.

Cell plasticity is central to maintaining the intricate equilibrium of the stem cell niche. Under stressful conditions, cells at the tip of the testis can dedifferentiate or transdifferentiate in order to maintain homeostasis. For example, GSCs can be replenished through spermatogonial dedifferentiation (Herrera & Bach, 2018). Additionally, hub cells can convert to the CySC population under both cell autonomous and non-autonomous contexts (Greenspan et al., 2022; Greenspan & Matunis, 2018; Herrera et al., 2021; Hétié et al., 2014; Voog et al., 2014). Cyst stem cells can contribute to the hub cell population under specific circumstances, such as genetic perturbation, although the frequency of this occurrence under normal physiological conditions remains unclear (DiNardo et al., 2011; Voog et al., 2008). While much work has been done to identify the key factors that dictate these processes, due to the highly context dependent nature of these events, many details remain to be revealed.

Our lab is interested in the molecular logic that governs cell fate decisions. Previous investigations revealed the transcriptional regulator Escargot (Esg) to be a major contributor in regulating the maintenance and behavior of both hub and CySC populations. Intrigued by the plasticity of these two functionally distinct cell types, this project aspires to further understand how Escargot balances hub and CySC fate.

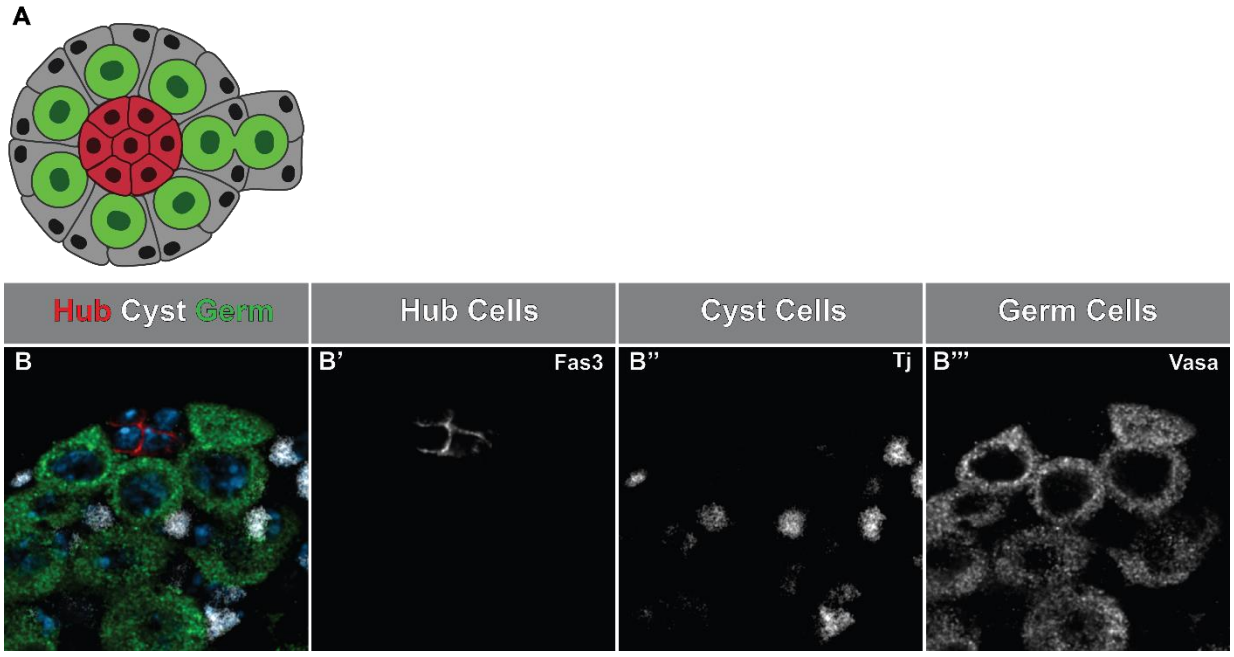

Figure 1: Overview of Testis Stem Cell Niche. (**A**) Hub cells (Red) provide essential signals and physical support that regulates and sustains the activities of both germline stem cells (Green) and somatic cyst stem cells (Gray). (**B**) Immunofluorescence image of the testis apex with all three cell types labeled. (**B'**) The membrane of hub cells is marked by an antibody targeting Fasciclin-3 (*Fas3*). (**B''**) The nuclei of early cyst cells are marked by an antibody targeting Traffic Jam (*tj*). (**B'''**) The cytoplasm of germ cells is marked by an antibody targeting Vasa (*vas*).

Escargot regulates cell fate in *Drosophila.*

Escargot (Esg) is a Snail family transcription factor that is an important cell fate determinate in many *Drosophila* tissues, such as brain, trachea, intestine, and testis(Korzelius et al., 2014; Loza-Coll et al., 2014; Miao & Hayashi, 2016; Sênos Demarco et al., 2022; Tanaka-Matakatsu et al., 1996; Whiteley et al., 1992; Yagi & Hayashi, 1997). Our lab has focused on the role of Escargot in the posterior midgut epithelium and apical testis niche, where *esg* expression

restricted. We have found that Escargot is an essential component in maintaining intestinal stem cells (ISCs) in the posterior midgut as well as hub cells and cyst stem cells in the testis. However, the mechanism(s) by which Esg influences cell behavior varies between the cell types, appears to be highly context specific, and remains to be fully understood.

In the fly intestine, Escargot expression is restricted to the ISCs and their progenitors, the enteroblasts (EB). Escargot maintains ISC stemness by repressing differentiation-promoting factors (e.g., *Pdm1*) and modulating regulators of Notch signaling (*Amun*). Loss of *esg* leads to rapid differentiation of ISCs, while forced expression of *esg* prevents differentiation (Korzelius et al., 2014; Loza-Coll et al., 2014). Furthermore, removing *esg* biases differentiation of ISC progenitors to favor the enteroendocrine (EE) lineage over enteroendocrine (EC), which normally shares an equal probability with the EEs (Loza-Coll et al., 2014). This suggests that Escargot plays a role in both maintaining ISCs and in directing the differentiation of the progenitors.

In the testis, Escargot expression is restricted to hub cells, CySCs, and early germ cells. It plays a crucial role in the autonomous maintenance of both hub cells and CySCs, but it is not necessary for GSC maintenance (Voog et al., 2014). Escargot maintains CySC fate by upregulating an insulin agonist, ImpL2, to suppress Insulin Receptor (InR) pathway activity and prevent differentiation. Indeed, overexpression of *esg* in CySCs represses InR signaling and inhibits differentiation, leading to an accumulation of CySC-like cells at the testis tip. Additionally, loss of *esg* function in CySCs promotes InR signaling, leading to a precocious differentiation of CySCs into cyst cells (Sênos Demarco et al., 2022). Similarly, hub cells lacking functional Esg are not maintained and convert into phenotypically normal CySCs (Voog et al., 2014). However, the mechanism by which Esg regulates hub cell fate has yet to be determined. Interestingly, clonal

analysis revealed that CySCs expressing hypermorphic alleles of *esg* sometimes generate abnormal hub cells (Voog et al., 2008), suggesting Esg might play a more nuanced role in somatic cell fate determination than is currently understood.

Escargot is differentially expressed in somatic cells.

Previous studies revealed the importance of *esg* expression levels in regulating somatic cell behavior. However, our understanding of the homeostatic levels of Esg protein in the testis was limited. To reliably detect Escargot protein, we generated a fly line that introduced an mCherry fluorescent tag at the N-terminus of the endogenous Escargot protein (henceforth referred to as Esg::mCherry). Immunostaining of young flies homozygous for the *esg::mCherry* allele revealed that Escargot protein was restricted to the testis apex. Escargot was consistently observed in hub and CySCs, while sporadically present in GSC/GBs (Figure 2B). These findings were consistent with the observations made using the commonly utilized *esg-GFP* enhancer-trap line. Nonetheless, the utilization of Esg::mCherry provided us with a more nuanced understanding of the variations in Esg levels across the different cell populations. Notably, hub cells had a significantly higher Esg::mCherry protein signal compared to any other cell type at the testis tip. Though Esg::mCherry was observed in CySCs, its concentration was much lower than in hub cells.

The differential expression of Escargot between hub cells and CySCs corroborates previous functional data that demonstrated the impact of altering Escargot levels on somatic cell behavior. Together, these findings support a model where Escargot serves as a central regulator of somatic cell fate. However, since Escargot transcriptionally regulates numerous targets, it is likely that it does not achieve this sophisticated balance of somatic cell fate through a single mechanism, but

rather through the coordination of multiple signals. In the next chapter, we present evidence highlighting one of the key genetic interactions responsible for balancing CySC and hub cell fates.

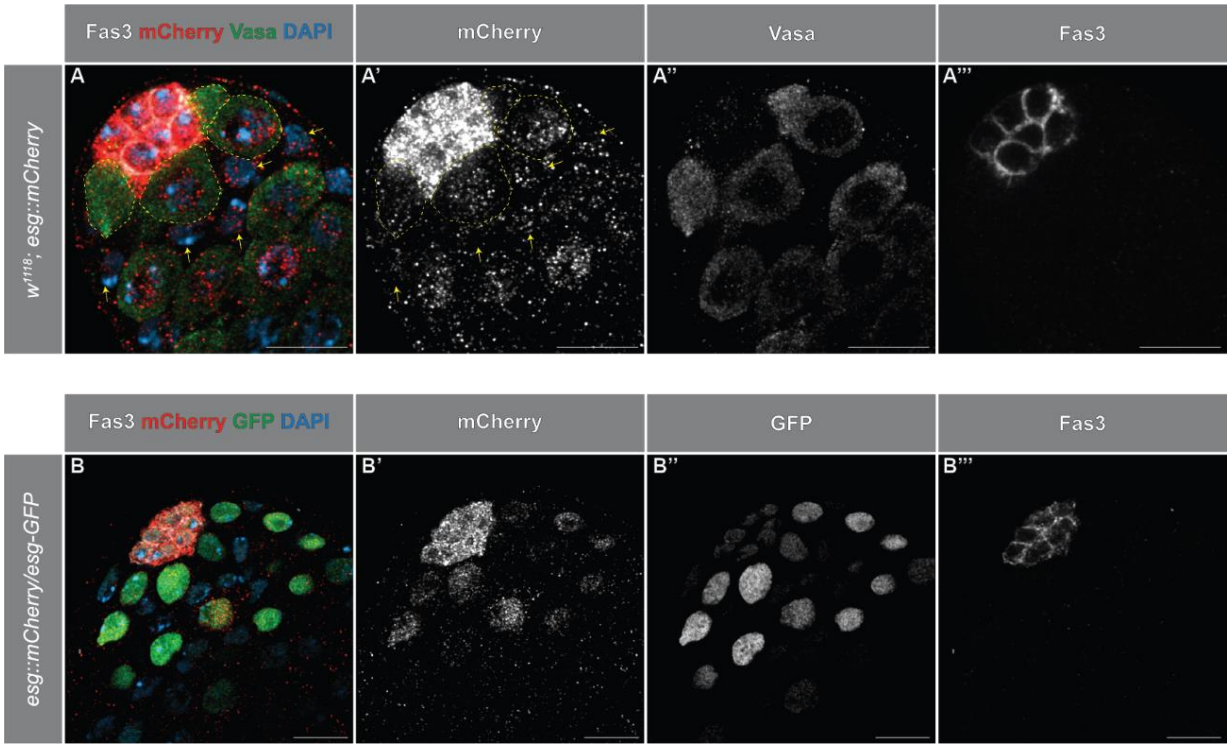

Figure 2: Escargot expression at the testis tip. (**A**) Representative image of a testis from flies homozygous for the *esg::mCherry* fusion allele. GSCs are outlined with a dotted yellow line. Yellow arrows point to Esg+ cyst cells. (**A'''**) Hub cell membranes are outlined by Fasciclin-3; (**A''**) the cytoplasm of germ cells are marked by Vasa. (**A'**) The Esg::mCherry fusion protein is targeted using an anti-mCherry antibody. (**B**) Representative image of a testis from flies with both *esg::mCherry* and the *esg-GFP* enhancer trap. (**B'**) mCherry signal marks cells positive for Escargot protein. (**B''**) GFP signal marks cells where an *esg* enhancer is active.

Chapter 2: Escargot Attenuates Egfr Signaling to Influence Somatic Cell Fate

Egfr is low in hub cells.

We cross-referenced established cell fate regulators with our roster of presumed Esg target genes, derived from our previously described DamID dataset (Sênos Demarco et al., 2022). In this analysis, Egfr was identified a putative target of Esg-mediated regulation, with significant Esg-Dam binding signal at the *Egfr* locus (Figure 3A). We decided to investigate the potential role of Egfr in Esg-mediated regulation because Egfr plays a pivotal role in controlling somatic cell fate during gonad niche development. Both cyst cells and hub cells stem from Somatic Gonadal Precursor cells (SGPs), and the lineage they adopt hinges on Egfr activity. Hub cells originate from SGPs exhibiting low Egfr activity, while SGPs featuring active Egfr commit to the cyst lineage (Kitadate & Kobayashi, 2010). This relationship remains consistent through adulthood, there is a significant contrast between hub cells and cyst cells when we visualize Egfr protein levels with an endogenously tagged *Egfr* (Figure 3B). When we compared this to the distribution of Esg::mCherry protein, we noticed an inverse relationship between Esg and Egfr protein levels at the testis apex. Opposing Escargot and Egfr relative protein levels prompts us to inquire whether Escargot influences the Egfr/MAPK pathway to regulate somatic cell behavior.

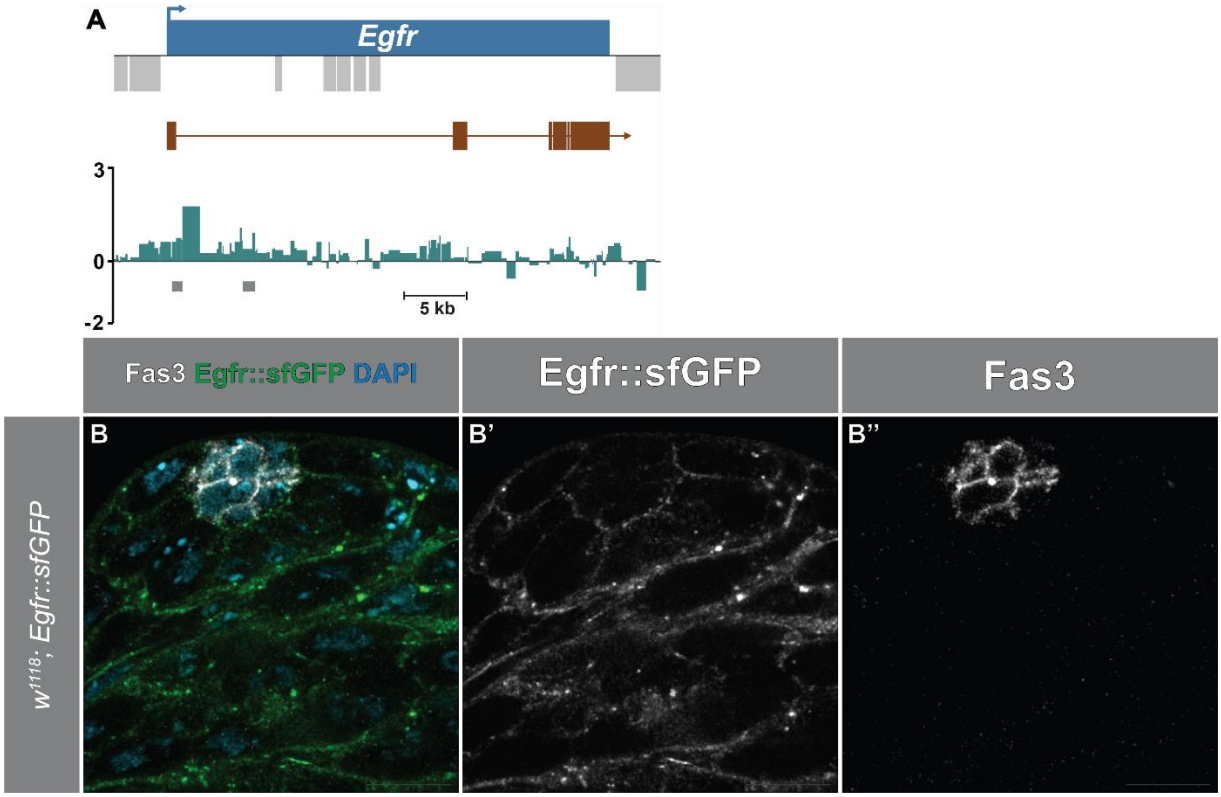

Figure 3: Egfr is a putative target of Esg and differentially expressed at testis tip. (**A**) Averaged plot of Esg-Dam occupancy from three independent biological sample pools. Gene body for Egfr is represented in blue, with exons represented in brown. Light gray boxes display additional genes. Esg-Dam occupancy is displayed below in teal. Significant binding sites are represented by dark gray rectangles under the plot. The Y axis represents the log2 ratio of Esg-Dam over Dam alone. (**B**) Representative image of a testis from flies homozygous for the *Egfr::sfGFP* fusion gene. Signal for Egfr::sfGFP is observed in all cell types at the tip of the testis, with the lowest signal residing in hub cells.

Depleting *esg* transcript from hub cells increases MAPK activity.

Given that the removal of Escargot from hub cells results in their conversion to CySCs, we expected that *esg* depletion would lead to an elevation in MAPK (Erk) activity. To test this, we introduced a transgenic reporter to measure Erk activity changes resulting from *esg* knockdown in hub cells. We expressed our UAS-controlled transgenes specifically in hub cells with an upd-GAL4 'driver' line and achieved temporal specificity by raising the crosses in the presence of a temperature-sensitive GAL80 (hereafter, upd^{TS}). We utilized the MAPK activity reporter, Erk-nKTR, which measures MAPK activity by comparing the nuclear signal of two equimolar fluorophores. When MAPK is inactive, both fluorophores localize to the nucleus. However, active MAPK leads to GFP exclusion from the nucleus, while RFP remains unchanged. As these fluorophores are produced in equal amounts, changes in MAPK activity are reflected in the nuclear RFP signal-to-GFP signal ratio (R/G) (Yuen et al., 2022). In the context of *esg* depletion alongside the Erk-nKTR reporter, we observed an increase in the average R/G ratio per cell, indicating an elevated MAPK activity (Figure 4B & 4D). We confirmed this observation with another approach. The MAPK activity sensor Erk-SPARK incorporates a GFP fused with a phase-separation domain. Upon activation, Erk phosphorylates the probe, inducing a phase-separation event that manifests as bright GFP puncta (Zhang et al., 2018). The depletion of *esg* alongside the Erk-SPARK reporter produced noticeable differences in GFP puncta, indicating heightened MAPK activity (Figure 4G). Collectively, this data supports the hypothesis that Escargot suppresses MAPK activity in hub cells under normal conditions.

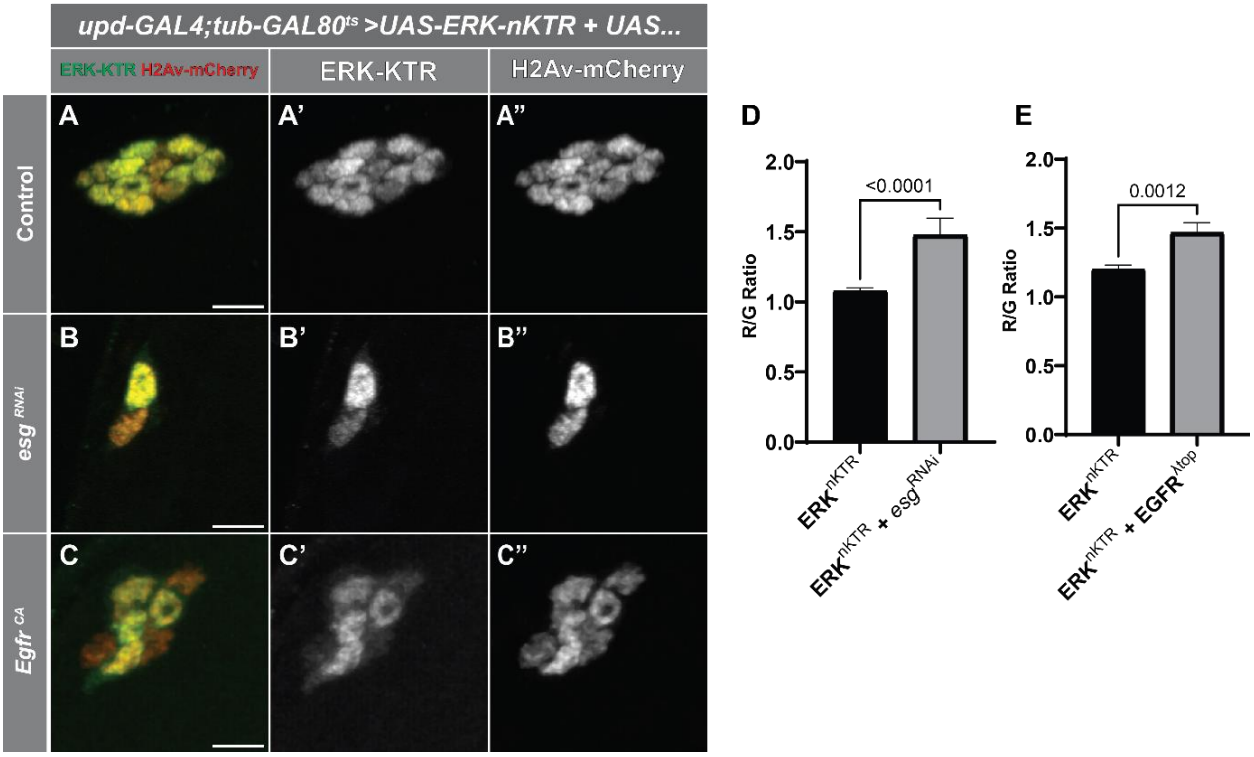

Figure 4: MAPK activity increases with *esg* depletion. (**A-C**) Representative images of hub cells from animals expressing (**A**) UAS-*ERK-nKTR*, (**B**) UAS-*ERK-nKTR* + UAS-*esg*$^{\text{RNAi (GD1437)}}$ and (**C**) UAS-*ERK-nKTR* + UAS-*Egfr* $^{\lambda\text{top}}$ for 5 days at 29°C. (scale bar: 5 μm) (**E**) Quantification of ERK-nKTR observations shown in (A)-(C). Hub cell nuclei were manually segmented in FIJI and stored in the ROI-manager. Then, the average intensity of both red and green channels was measured per nuclei and reported as a ratio (Red/Green), as described in Yuen et al., 2022. Since the nuclear mCherry protein is equimolar to the Erk-KTR sensor, we can quantify changes in ERK activity by calculating how much green signal is absent from the nucleus. Statistical significance was calculated with student t-test with at least n=40 hub cells per genotype. Error bars represent SEM.

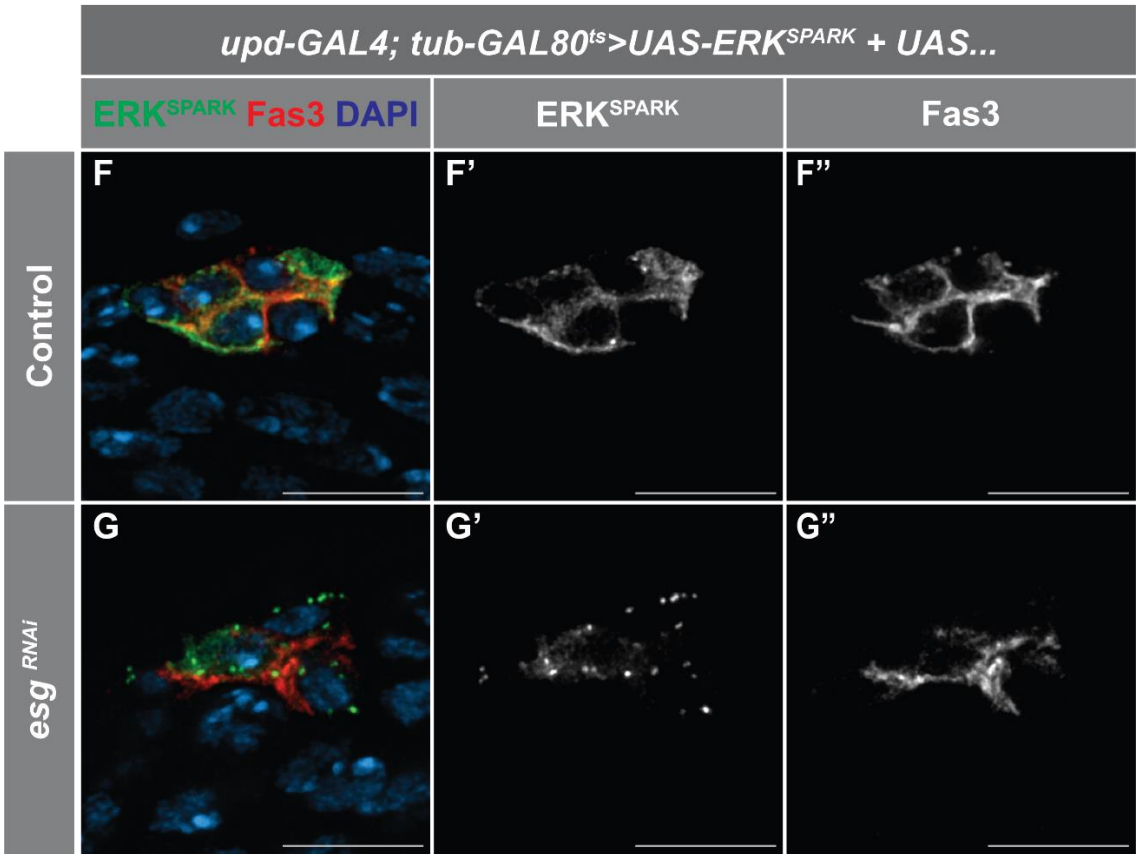

Figure 4: MAPK activity increases with *esg* depletion. (**F-G**) Representative images of hub cells from animals expressing (**F**) UAS-ERK-SPARK and (**G**) UAS-*esg*$^{\text{RNAi (TRiP.HMS02538)}}$ + UAS-ERK-SPARK for 5 days at 29°C. (scale bar: 10 μm)

Escargot attenuates Egfr/MAPK pathway to maintain hub cell fate.

Since the removal of Esg from hub cells elevates MAPK activity, we hypothesized that suppression of Egfr activity is vital for the preservation of hub cell identity. To explore this, we investigated whether the inhibition of Egfr activity could mitigate the hub cell phenotypes triggered by *esg* depletion. The targeted reduction of *esg* in adult hub cells induces their transformation into CySCs and their commitment to the cyst cell lineage, consequently leading to a gradual decline in the number of hub cells (as depicted in Figures 5A-B). However, the inhibition

of Egfr (achieved through either the expression of a dominant-negative or by triggering RNAi) while *esg*^{RNAi} is in effect, prevents the loss of hub cells (Figure 5B-C). As depletion of *esg* transcript causes hub cells to convert into CySCs, we aimed to confirm that repressing Egfr in this context was preventing Hub-to-CySC conversion. To assay converting cells, we utilized the ReDDM lineage tracing method with the upd^{TS} driver (upd^{ReDDM}). In this system, real-time driver expression is marked by a transient GFP signal, while any differentiated progeny are traced by a persistent H2B::RFP signal (Antonello et al., 2015). In standard conditions, the GFP and H2B::RFP signals are restricted to hub cells exclusively (as shown in Figure 6A). However, upon the knockdown of *esg*, a significant increase in GFP-RFP+ cells distant from the hub are observed (Figure 6B), which aligns with previous observations using an alternative lineage tracing tool(Voog et al., 2014). When we co-expressed a dominant-negative Egfr (Egfr^{DN}) along with *esg*^{RNAi} using upd^{ReDDM}, a substantially reduced incidence of Hub-to-CySC conversion is observed compared to cases involving *esg*^{RNAi} alone (Figure 6B-C). These findings provide compelling evidence that Escargot preserves the identity of hub cells by inhibiting the activity of the Egfr pathway.

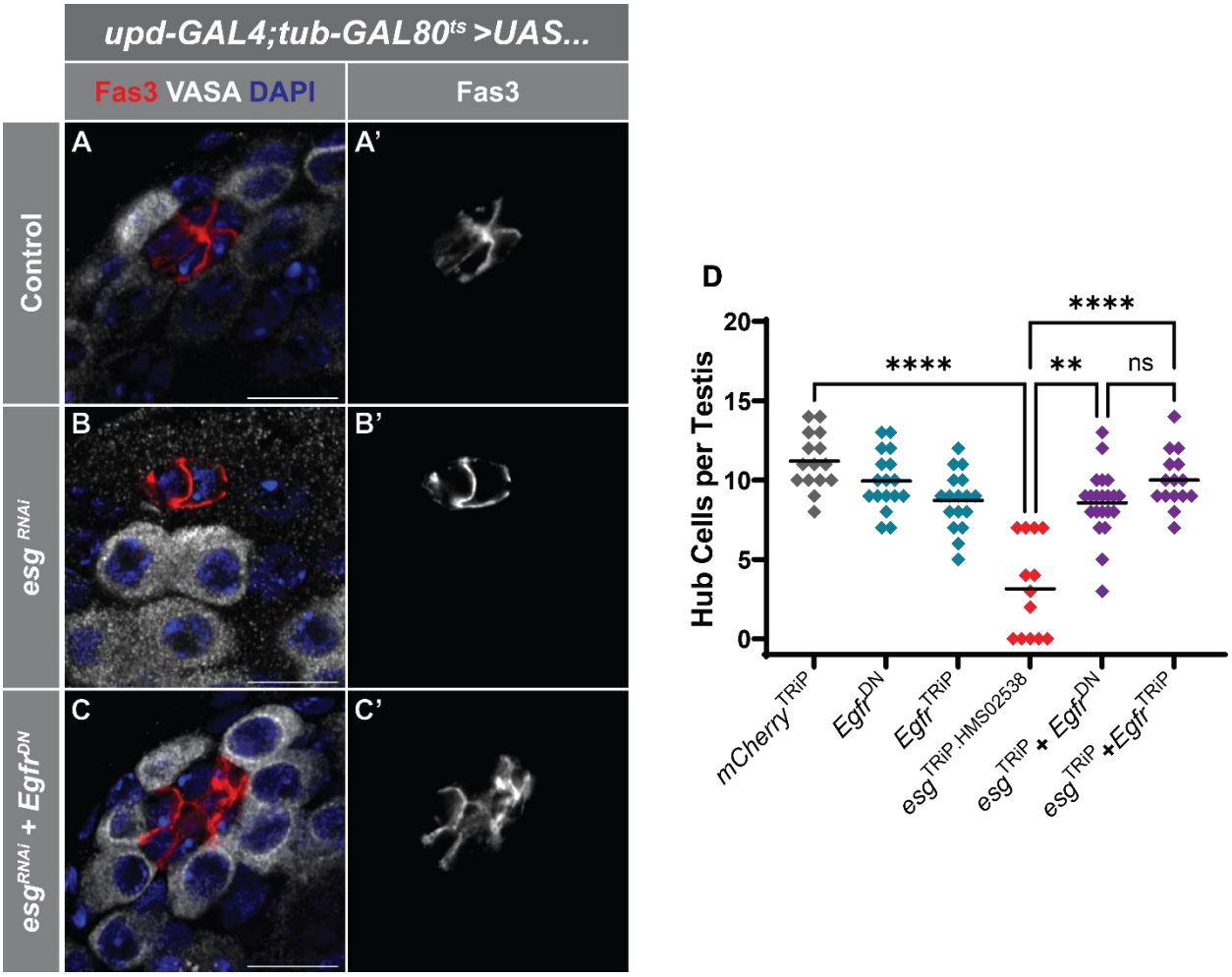

Figure 5: Escargot loss of function rescued by suppressing Egfr in hub cells. (**A-D**) Fixed testes samples were prepped for immunofluorescence microscopy, using an anti-Fas3 antibody to mark hub cells, anti-VASA antibody to mark germ cells, and DAPI dye to mark all nuclei. Representative images here were taken on an LSM 880 confocal microscope. (**A**) Representative image of upd^{TS}> $UAS\text{-}mCherry^{RNAi}$ (**B**) Representative image of upd^{TS}> $UAS\text{-}esg^{RNAi\text{-}(TRiP.HMS02538)}$ (**C**) Representative image of upd^{TS}> $UAS\text{-}esg^{RNAi}$ + $UAS\text{-}Egfr^{DN}$ (**D**) Quantification of remaining hub cells per testis after 10 days, per condition. Statistical significance was calculated using nonparametric ANOVA.

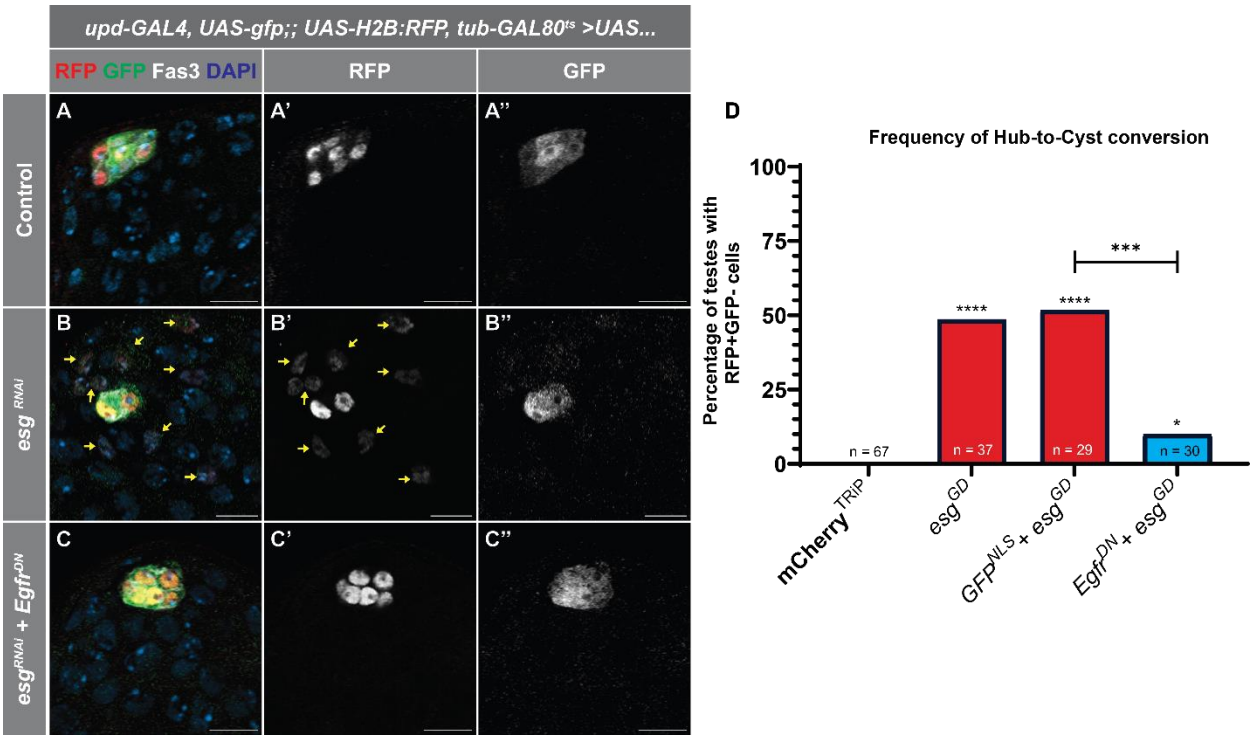

Figure 6: Inhibiting Egfr suppresses hub-to-CySC conversion. (**A-D**) Fixed testes samples were prepped for immunofluorescence microscopy, using an anti-Fas3 antibody to mark hub cells, anti-GFP antibody to mark cells currently expressing GAL4, anti-DsRed to mark cells that have H2B::RFP, and DAPI dye to mark all nuclei. Representative images here were taken on an LSM 980 confocal microscope. Scale bar: 10µm (**A**) Representative image of upd^{ReDDM}> *UAS-mCherry*^{RNAi} (**B**) Representative image of upd^{ReDDM} > *UAS-esg*$^{RNAi\ (GD1437)}$. Yellow arrows point to H2B::RFP+ nuclei from cells no longer expressing hub cell biomarkers (GFP, Fas3). (**C**) Representative image of upd^{ReDDM} > *UAS-Egfr* ^{DN}+*UAS- esg*$^{RNAi\ (GD1437)}$ (**D**) Contingency plot displaying the frequency at which H2B::RFP-positive, GFP-negative nuclei were observed across tested genotypes. Statistical significance was determined by conducting a two-sided Fisher's exact test on the raw data between each genetic manipulation and control sample (upd^{ReDDM}> *UAS-mCherry*^{RNAi})

Egfr/MAPK pathway activation in hub cells drives them to convert into CySCs.

Since our data suggests that Esg represses Egfr activity to prevent precocious Hub-to-CySC conversion, we questioned if ectopic Egfr pathway activity was sufficient to induce Hub-to-CySC conversion. Indeed, upon expressing a constitutively active Egfr variant in adult hub cells via upd^{TS} over a period of 10 days, we observed a decrease in the average count of hub cells per testis. Similar outcomes were noted when we induced ectopic activation of the Egfr signaling pathway by expressing the hypermorphic *Ras85D* allele (*Ras^{V12}*) or *Pnt* under the same conditions (Figure 7A). Moreover, expressing hypermorphic *Egfr* or *Ras85D* alleles or *Pnt* with upd^{ReDDM} results in a notable increase in GFP-RFP+ cells away from the hub (Figure 7B). Hence, akin to the effects of *esg* knockdown, the activation of the Egfr cascade leads to the conversion of hub cells into CySCs. These results are consistent with findings reported recently with a different lineage tracing method (Greenspan et al., 2022). Echoing the developmental checkpoint mentioned earlier, the control of Egfr activity emerges as a critical factor in the maintenance of hub cells.

We confirmed the hub-to-CySC conversion induced from ectopic activation of the Egfr cascade was due to MAPK signaling and not a non-canonical pathway downstream of Egfr. We utilized two hypermorphic Ras effector loop mutants (Ras$^{V12, G37}$ and Ras$^{V12, S35}$) with impaired abilities to signal to cascades(Karim & Rubin, 1998). The Ras$^{V12, G37}$ mutant has an impaired ability to bind with Raf and PI3K and preferentially signals to Ral. The Ras$^{V12, S35}$ allele has normal affinity to Raf, so it will signal to MAPK, but has an impaired ability to signal to Ral and PI3K. When we expressed these mutants in hub cells for 10 days, only testes expressing the Ras$^{V12, S35}$ variant were observed to have an increased hub-to-CySC conversion frequency and fewer hub cells (Figure 8).

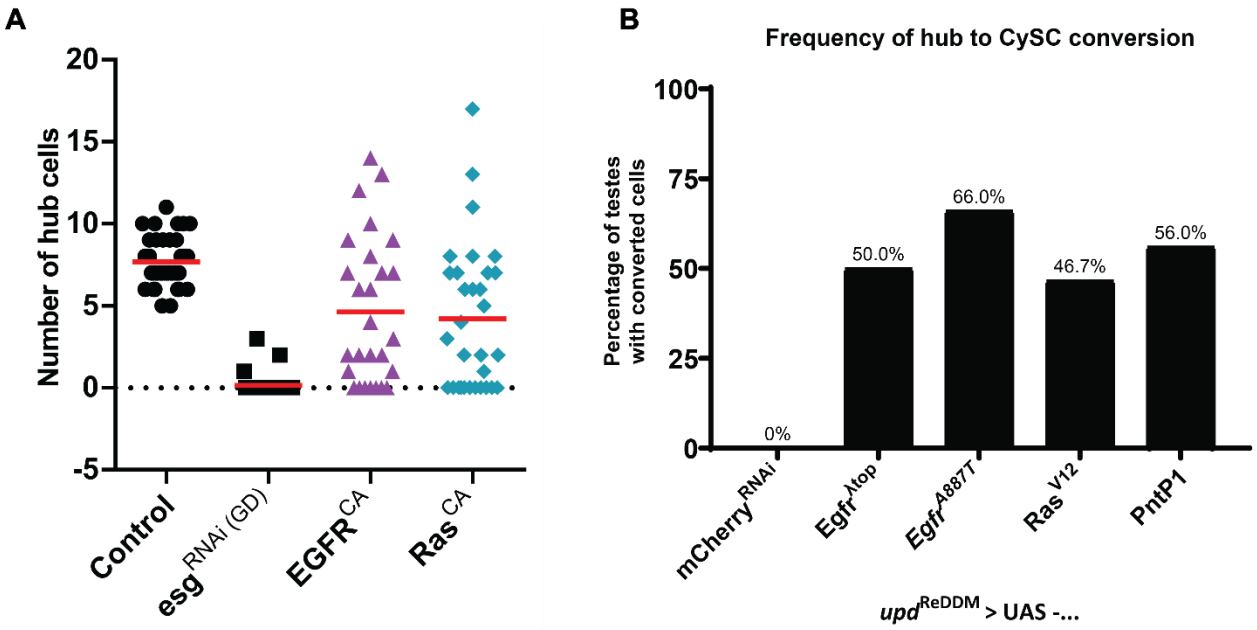

Figure 7: Hub cells are not maintained during ectopic Egfr pathway activation. (**A**) Number of hub cells per testis when *Egfr*$^{\lambda top}$ (EGFR^{CA}) or *Ras*^{V12} (Ras^{CA}) are expressed for 10 days with the upd^{TS} driver. (**B**) Hub-to-CySC conversion frequency when upd^{ReDDM} is used to express transgenes that activate the Egfr-MAPK signaling axis for 10 days.

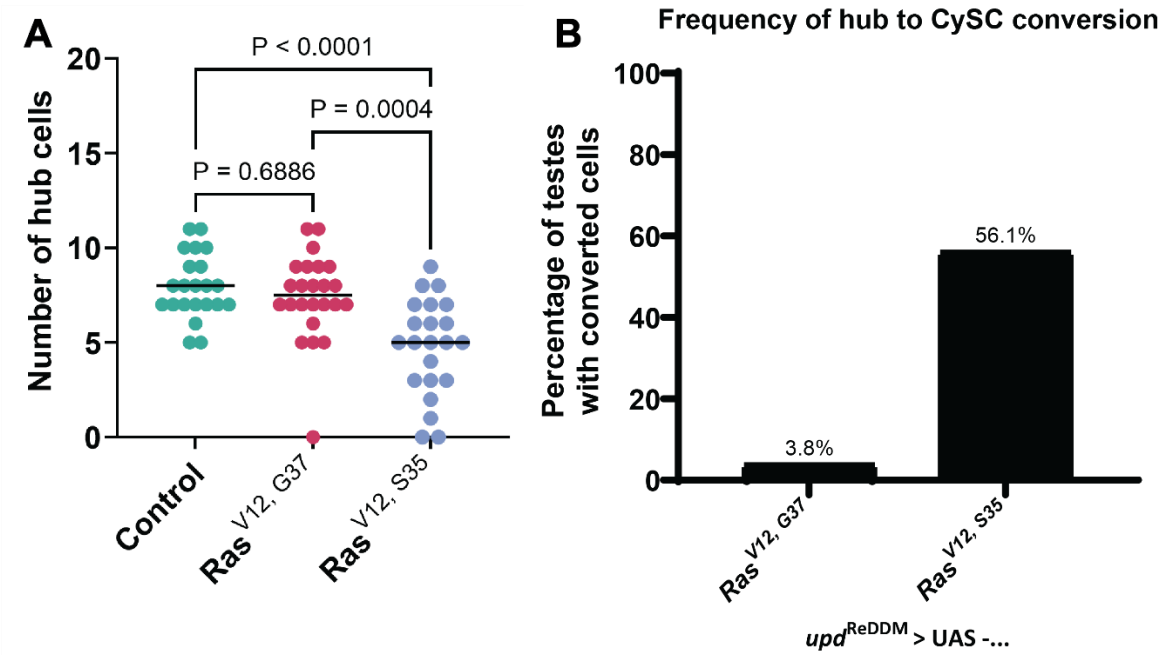

Figure 8: Ras effector loop mutants point to conversion being MAPK-dependent. (**A**) Quantification of hub cell numbers when Ras effector loop mutants are expressed in hub cells for 10 days using updTS driver. Statistical significance is determined with one-way ANOVA. (**B**) Hub-to-CySC conversion frequency when upd^{ReDDM} is used to express the effector loop mutants. Samples with $Ras^{V12, G37}$ exhibited less hub-to-CySC conversion (3.8%, 1 out of 26 samples) compared to samples with $Ras^{V12, S35}$ (56.1%, 23 out of 41 samples).

Hub cells do not reenter cell cycle upon *esg* loss of function.

Cellular quiescence is a defining characteristic of hub cells. Previous work has demonstrated that when hub cells are forced to reenter the cell cycle, they are no longer maintained as hub cells(Greenspan & Matunis, 2018; Hétié et al., 2014). Activating Egfr in hub cells also drives them out of quiescence (Greenspan et al., 2022). Given our data suggesting Esg maintains hub cell fate by repressing Egfr, we investigated whether hub cells enter the cell cycle when Esg is depleted.

We began our cell cycle analysis by performing an EdU (5-ethynyl-2'-deoxyuridine) incorporation assay to track cell cycle changes in hub cells during *esg* depletion or ectopic activation of the Egfr-MAPK pathway. EdU is a thymidine analog that gets incorporated into newly synthesized DNA during the S phase of the cell cycle and is visualized with a fluorescent azide. This method enables the identification and quantification of proliferating cells. We expressed esg^{RNAi}, $Egfr^{DN}$, or $Egfr^{\lambda top}$ in hub cells and dissected testes after 10 days, and incubated testes in the ClickIT EdU reaction solution for 30 minutes. We found no EdU incorporation in control or esg^{RNAi}-treated hub cells. However, one out of 20 hubs expressing $Egfr^{\lambda top}$ for 10 days contained cells that incorporated EdU, which is consistent with previously published work. However, since the cell cycle is a multi-phase process that occurs over several hours, we looked to broaden our detection range beyond cells in S-phase during the 30-minute incubation period (Figure 9E).

We used the FlyFUCCI (Fluorescent Ubiquitination-based Cell Cycle Indicator) tool to identify hub cells in G_0/G_1, S, or G_2/M phase. FlyFUCCI allows identification of cell cycle phase through the combination of two ubiquitously expressed fusion proteins: GFP::E2f1$_{(1-230)}$ to mark

G_0/G_1 phases and RFP::$CycB_{(1-266)}$ to mark S, G_2, and early M phases. We tracked the cell cycle phase by scoring hub cell nuclei for the presence of GFP, RFP, or both. We induced esg^{RNAi} or Ras^{V12} expression in hub cells and compared their cell cycle states to a control after 5 days. Control hub cells showed only GFP signals, indicating quiescence. Hub cells with esg^{RNAi} also showed no RFP signals, indicating they remained in G_0 (Figure 9A). Expressing Ras^{V12} in hub cells for 5 days was sufficient to drive some hub cells into S-phase (Figure 9C), which is consistent with previously published work, and confirms the tool's efficacy for measuring cell cycle changes in this cell type. Previous experiments in our lab have shown that overexpressing *esg* in CySCs leads to an accumulation of proliferative cells at the testis tip. As such, it makes sense that Esg is not directly involved with maintaining hub cell quiescence.

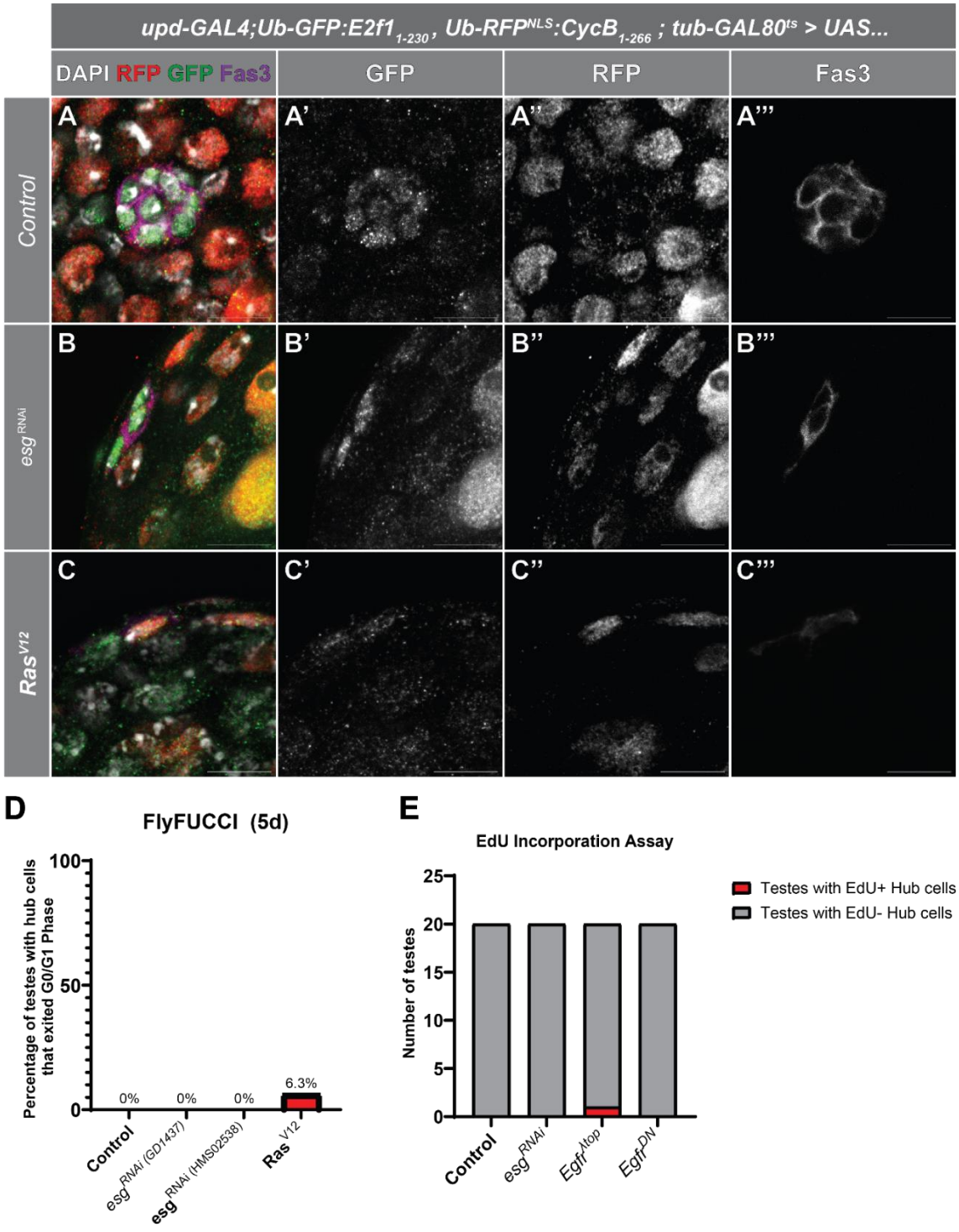

Figure 9: Cell cycle analysis during *esg* depletion. (**A-C**) Representative images from the FlyFUCCI experiment. (**A**) Hub cells in control testes (upd^{TS} w^{1118} outcross) show only GFP

signal, indicating G_0/G_1 status (20 out of 20 samples). (**B**) Hub cells treated with $upd^{TS}>esg^{RNAi\ HMS0258}$ for 5 days show only GFP signal, indicating G_0/G_1 status (10 out of 10 samples for each RNAi line). (**C**) Hub cell from a testis in the $upd^{TS}>UAS\text{-}Ras^{V12}$ condition displaying RFP signal, but not GFP, indicating it is in S-Phase (1 out of 15 samples). (scale bar: 10 μm) (**D**) Quantification of FlyFUCCI experiment showing the percentages for each condition. (**E**) Quantification of EdU incorporation assay. All transgenes were expressed with upd^{TS} for 10 days.

Egfr and Esg are important regulators of cyst cell behavior.

We previously reported that overexpressing Escargot in cyst cells results in an accumulation of early cyst cells, while depleting Escargot from cyst cells results in less early cyst cells (Sênos Demarco et al., 2022; Voog et al., 2008). Considering this, in conjunction with the conspicuous discrepancy in Escargot protein levels observed between hub cells and cyst cells (Figures 2A & 3B), our objective was to explore the hypothesis that Escargot protein levels play a pivotal role in determining the fate of somatic cells.

Egfr signaling has significant impacts on CySC and cyst cell behavior. Egfr signaling is essential for the proper differentiation of cyst cells(Kiger et al., 2000). Impaired signaling in cyst cells alters their ability to properly coordinate with the germline, leading to GB encapsulation defects or asynchronous TA divisions(Hudson et al., 2013). Additionally, our lab demonstrated that Egfr signaling maintains CySCs through stimulating autophagy to regulate lipid levels(Sênos Demarco et al., 2020). Furthermore, Egfr signaling has been shown to influence CySC competitiveness for niche occupancy(Amoyel et al., 2016; Lu et al., 2019). Since our data supports a model that Esg promotes hub cell maintenance through repressing Egfr pathway activity, we were interested if this relationship was the separating line between hub and CySC fates.

Overexpressing *esg* in CySCs/CCs promotes switch to hub cell fate.

Since Escargot protein is substantially higher in hub cells compared to cyst cells, we were curious if overexpressing Escargot in early cyst cells was sufficient to induce a CySC-to-hub fate change. To test this, we adapted the previously described ReDDM lineage tracing method to our cyst cell driver ($c587^{ReDDm}$). In adult testes, *c587* expression is confined to the early cyst cell lineage; hence, GFP signal is never observed in hub cells (Figure 10A). When we over expressed

Escargot with c587^{ReDDM}, a notable increase in H2B::RFP+ hub cells was evident across three distinct Esg overexpression constructs (Figure 10B-C), providing strong evidence that Escargot overexpression indeed prompts the conversion of some cyst cells into hub cells. Conversely, when we overexpressed *tj*, a gene with no discernible impact on cyst cell maintenance, there was no significant alteration in the number of H2B::RFP+ hub cells (Figure 10D).

CySCs are the sole mitotic somatic cell population at the testis apex and thus the only somatic cells that undergo homologous recombination. Taking advantage of this characteristic, we conducted a MARCM clonal analysis to overexpress Escargot (*esg*^{EP2009}) in single CySCs, rather than the entire population, as with c587^{ReDDM}. Our examination of GFP+ clones 7 days after heat-shock labeling revealed a substantial increase in GFP+Fas3+ cells in the *esg^{EP2009}* condition (Figure 11). This supports the hypothesis that Esg is controlling cell fate intrinsically, rather than altering the microenvironment such that conversion is driven by extrinsic factors.

Given that Escargot maintains hub cells by repressing Egfr activity, we aimed to assess whether manipulating Egfr activity could induce CySC-to-hub conversion. Upon expressing a dominant-negative Egfr with c587^{ReDDM}, we observed a significant increase in H2B::RFP+ hub cells compared to the control. However, the expression of a constitutively active Egfr using c587^{ReDDM} showed negligible variation in H2B::RFP+ hub cells, suggesting no notable rise in CySC-to-hub conversion occurrences. Intriguingly, the co-expression of constitutively active Egfr (*Egfr^{CA}*) and *esg^{EP2009}* yielded significantly fewer CySC-to-hub conversion events (Figure 10D). These observations parallel earlier findings and support the hypothesis that Escargot influences somatic cell identity through modulation of the Egfr signaling cascade.

These observations indicate that increasing Escargot levels in cyst cells suffices to redirect their fate towards adopting hub cell characteristics. This outcome concurs with the notion that Escargot levels hold a pivotal role in defining somatic cell identity within the adult testes. Furthermore, it aligns with observations made under homeostatic conditions, in which Escargot protein levels are substantially higher in hub cells than cyst cells.

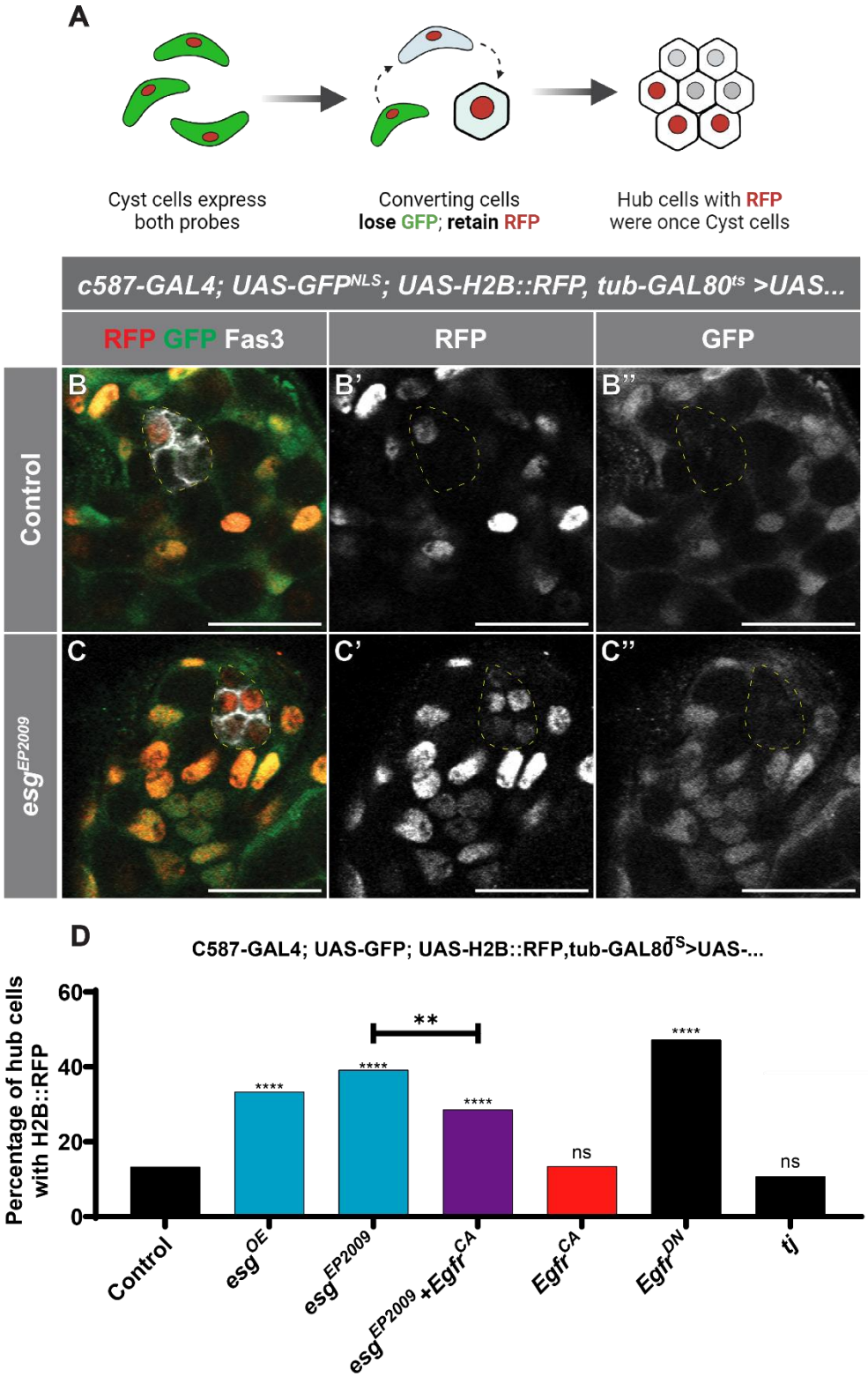
A
Cyst cells express both probes
Converting cells lose GFP; retain RFP
Hub cells with RFP were once Cyst cells
c587-GAL4; UAS-GFPNLS; UAS-H2B::RFP, tub-GAL80ts >UAS...
RFP GFP Fas3
RFP
GFP
Control
esgEP2009
B
B'
B''
C
C'
C''
D
C587-GAL4; UAS-GFP; UAS-H2B::RFP,tub-GAL80TS>UAS-...
Percentage of hub cells with H2B::RFP
60
40
20
0
**
****
****
****
ns
****
ns
Control
esgOE
esgEP2009
esgEP2009+EgfrCA
EgfrCA
EgfrDN
tj

Figure 10: Escargot represses Egfr to direct somatic cell fate. All transgenes were crossed to an c587-GAL4; UAS-*GFP*^{NLS}; UAS-H2B:RFP, tub-GAL80^{ts} (c587^{ReDDM}) driver line to restrict their expression to CySCs and early cyst cells of adult testes. Adult males were shifted from inhibitory temperature 18°C to the permissible temperature of 29°C for 7 days. Fixed testes samples were prepped for immunofluorescence microscopy, using an anti-Fas3 antibody to mark hub cells, anti-GFP antibody to mark cells currently expressing GAL4, anti-DsRed to mark cells that either currently are, or once were, expressing GAL4, and DAPI dye to mark all nuclei. Representative images here were taken on an LSM 980 confocal microscope. Scale bar: 10μm (**A**) Simplified schematic to visualize the CySC-to-hub conversion assay. (**B**) Representative image of w^{1118} outcross after 7 days at 29°C. RFP+GFP- nuclei are occasionally observed in the Hub (Fas3+) (**C**) Representative image of the niche after 7 days of *esg* overexpression (*esg*^{EP2009}). A significant amount of Fas3+RFP+GFP- cells are observed. (**D**) Quantification of percentage of hub cells with RFP+GFP- cells after 7 days of expressing the transgenes in CySC/early cyst cells. Statistical significance was determined by Fisher's exact test. Number of hub cells assayed per condition are: Control, n=662; *esg*^{EP2009}, n=592; *Egfr*^{DN}, n=432; *Egfr*$^{\lambda top}$, n=415; *esg*^{EP2009}+*Egfr*$^{\lambda top}$, n=210

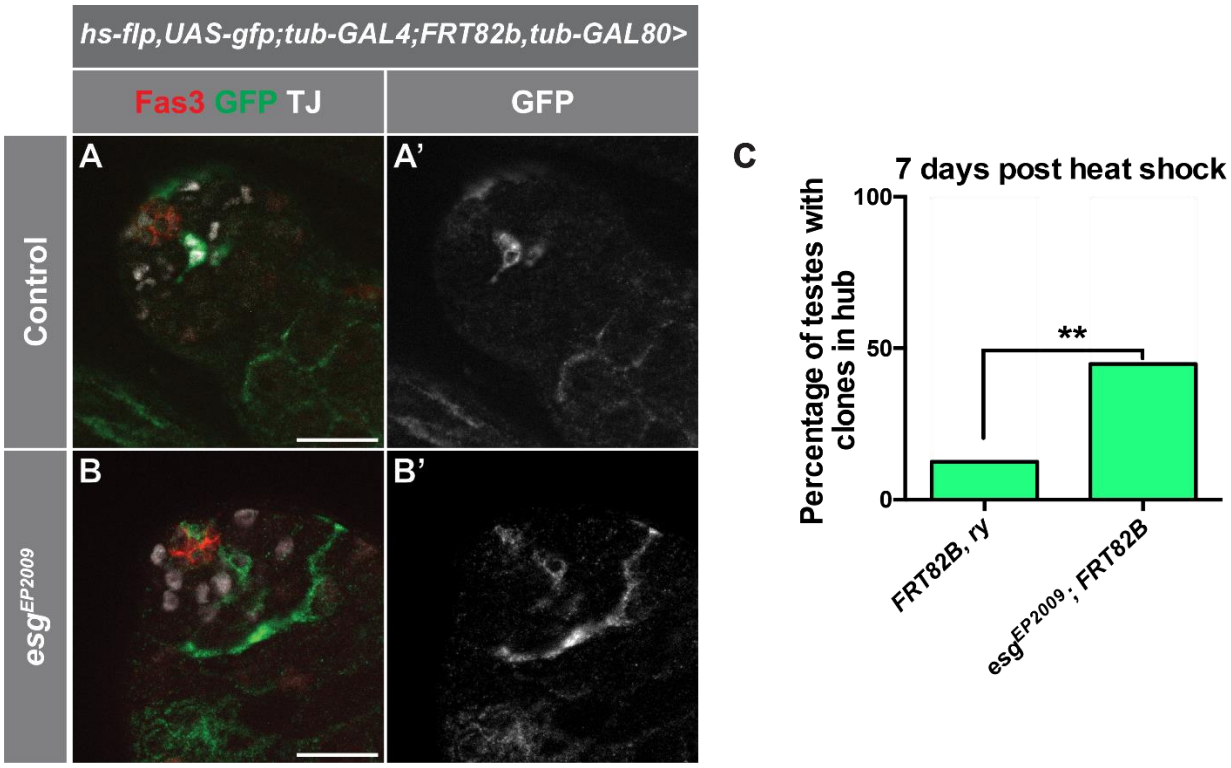

Figure 11: Individual CySCs overexpressing Escargot convert to hub cells. Representative images of MARCM clonal analysis in (**A)** Control testes (FRT82B,ry) and (**B**) testes with CySC clones expressing *esg*^{EP2009}. (**C**) Quantification of results. Statistical significance was determined by Fisher's exact test.

Somatic cell conversion frequencies change with age.

We have previously reported that *esg* transcript at the testis tip declines with age. Additionally, minor declines in hub cell number have also been observed with age (Boyle et al., 2007; Herrera et al., 2021; Wallenfang et al., 2006). We confirmed that the transcript declined with age as well as protein. We wanted to assess if this decline in *esg* transcript drives any age-related phenotypes at the testis tip. Since Esg protein levels decline with age, we hypothesized MAPK activity would increase in hub cells, there to be more hub-to-CySC conversion and less CySC-to-hub conversion.

Using lineage tracing tools, we assessed somatic cell conversion frequency as flies age (Figure 13). Four-week-old flies (29°C) showed a marked increase in hub-to-CySC conversion frequency (Figure 13A). Despite this increase, the total number of hub cells per testis did not significantly change, consistent with previous reports (Figure 13C). Current data suggest elevated MAPK activity (measured by Erk-nKTR) in aged hub cells (Figure 12D), though further validation is needed due to uneven expression of the Erk-nKTR transgene in aged hub cells.

CySC-to-hub conversion frequency declines in aged testes. Initially, it seems to plateau after 14 days at 29°C (Figure 13B). However, this approach does not specify when during the incubation period the conversion occurred, only that it happened at some point. Hence, we aged flies for 30 days without lineage tracing probes, then activated the tracing system by shifting them to 29°C for 3 days (Figure 13B). In this context, conversion was significantly less than in younger flies, indicating less frequent CySC-to-hub conversion in aged tissue.

Collectively these results support the model that declining levels of Esg at the tip of the testis reduces somatic cell plasticity. Although we did not observe a large shift in total number of

hub cells at the testis tip with age, it has been reported that number of GCSs decline with age(Boyle et al., 2007; Wallenfang et al., 2006). GCSs rely on hub cells for their stemness (Kiger et al., 2001). Thus, one possibility is that although the age-related decline of *esg* expression does not invoke a severe cell fate phenotype, it still has an impact on hub cell function. Most Escargot studies have focused on what happens when *esg* transcript is dramatically altered. While this approach has illuminated the dynamics of somatic cell behavior in the testis, it only informs us on what happens in extreme scenarios and may not be relevant to the normal physiological fluctuations in Esg activity. Indeed, since Esg has many targets, there likely is a spectrum of phenotypes that correspond to more modest changes in Esg abundance.

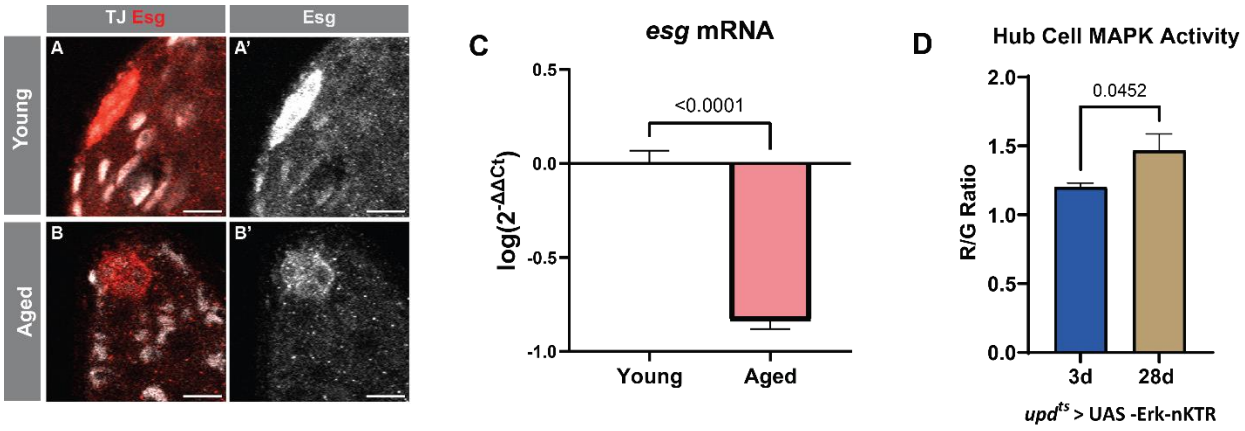

Figure 12: Escargot levels decline with age while MAPK activity increases. Representative images from of testis tips from (**A**) Young and (**B**) Aged flies expressing *esg::mCherry*. (**C**) Quantified levels of *esg* mRNA between Young and Aged whole testes. (**D**) Preliminary quantification of changes in MAPK activity (upd^{TS}>UAS-Erk-nKTR) in hub cells of aged testes compared to young.

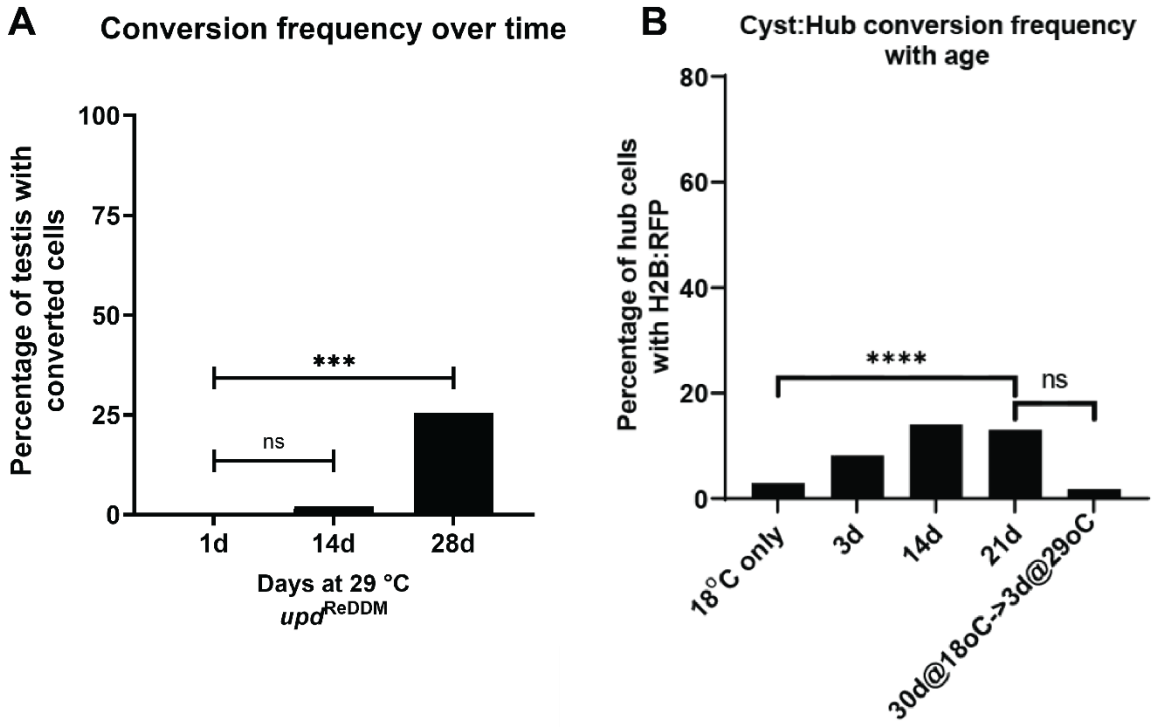

Figure 13: Somatic cell conversion frequency changes with age. (**A**) Hub-to-CySC conversion frequency when upd^{ReDDM} is crossed to w^{1118} and shifted to 29°C for 1, 14, or 28 days. (**B**) CySC-to-Hub conversion frequencies when c587^{ReDDM} and shifted to 29°C for 3, 14, or 21 days or when flies of the same genotype were aged for 30 days with the lineage tracing system suppressed and subsequently expressed for 3 days at 29°C.

The number of hub cells dramatically changes prior to adulthood.

Hub cell conversion to CySCs appears to be an infrequent occurrence in standard conditions. Even with age, we only see evidence of conversion in about 25% of testes (Figure 13A). Since it is an infrequent natural occurrence in adulthood, we were curious in which physiological contexts hub-to-CySC conversion happened, if any.

During the maturation of the testis the size of the hub dramatically changes. Clusters of hub cells found in third instar larvae (hereafter, L3) can be as large as 40 cells, with an average of around 21 in our experiments, while hub clusters of newly eclosed flies are about half the size of their L3 counterparts (Figure 14). Previous experiments in our lab indicate this reduction in hub size is mediated by hub-to-CySC conversion(Voog et al., 2014). Hence, we wanted to test the hypothesis that this hub-to-CySC conversion is coordinated by Esg and Egfr signaling.

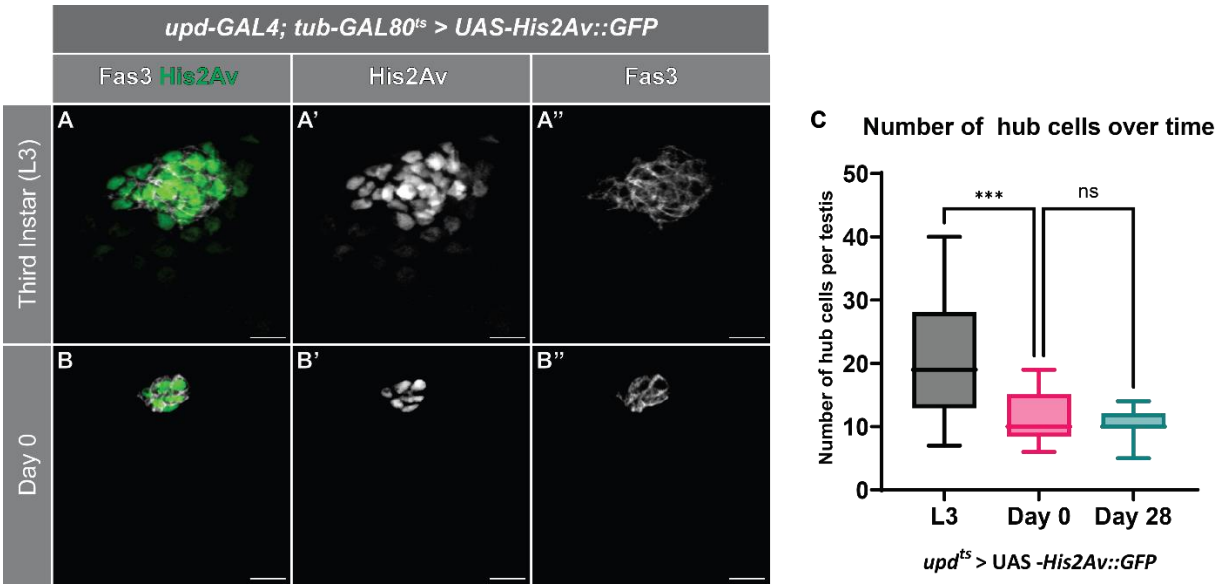

Figure 14: Hub size dramatically changes during development. Representative images depicting hub populations from (**A**) third instar (L3) testes and (**B**) Newly eclosed (Day 0) adult testes. (**C**) Quantification of average number of hub cells between L3, Day 0, Day 28 samples.

Modulating *esg* or *Egfr* do not impact hub cell reduction during development.

If the remodeling of hub size was due to coordinated hub-to-CySC conversion, we hypothesized that overexpressing *esg* or $Egfr^{DN}$ with the upd^{ReDDM} driver would be sufficient to repress it. We raised the flies at 18°C until the start of stage L3 and subsequently shifted them to 29°C to initiate the transgene expression. This allowed us to bypass any adverse developmental effects, since previous experiments struggled when raised at 29°C. Testes were dissected on the day of eclosion to quantify the frequency of hub-to-CySC conversion.

Our results indicated that there was no significant difference in the number of hub cells between the experimental conditions and the control group (Figure 15A). Specifically, the average number of hub cells in the control group was 12.59 (n = 70), while the esg^{EP2009}, $Egfr^{DN\#1}$, $Egfr^{DN\#2}$ overexpression groups had averages of 13.03 (n = 70), 13.22 (n = 23), and 12.24 (n = 21), respectively.

Furthermore, neither *esg* overexpression nor repression of Egfr activity significantly influenced the frequency of hub-to-CySC conversion (Figure 15B). Although we did observe less frequent hub-to-CySC conversion when we overexpressed *esg* (6 out of 39 samples,15.4%) compared to the outcross control (16 out of 65 samples, 24.6%), this was not a statistically significant result. Meanwhile, expressing either $Egfr^{DN\#1}$ or $Egfr^{DN\#2}$ seemed to have an even less potent effect (5 out of 18 samples, 27.8%; 3 out of 17 samples, 17.6%, respectively).

Further experiments are necessary to confirm these findings. For example, a critical control involves raising flies of the same genotype at 18°C, where transgenes are inactivated, to ensure that any observed differences in hub cell numbers are not due to inherent genetic background variability. If expressing esg^{EP2009} or $Egfr^{DN}$ is suppressing the hub-to-CySC conversion during

this developmental timepoint, then the average hub size for the 18°C of the same genotype will be larger than what is reported here.

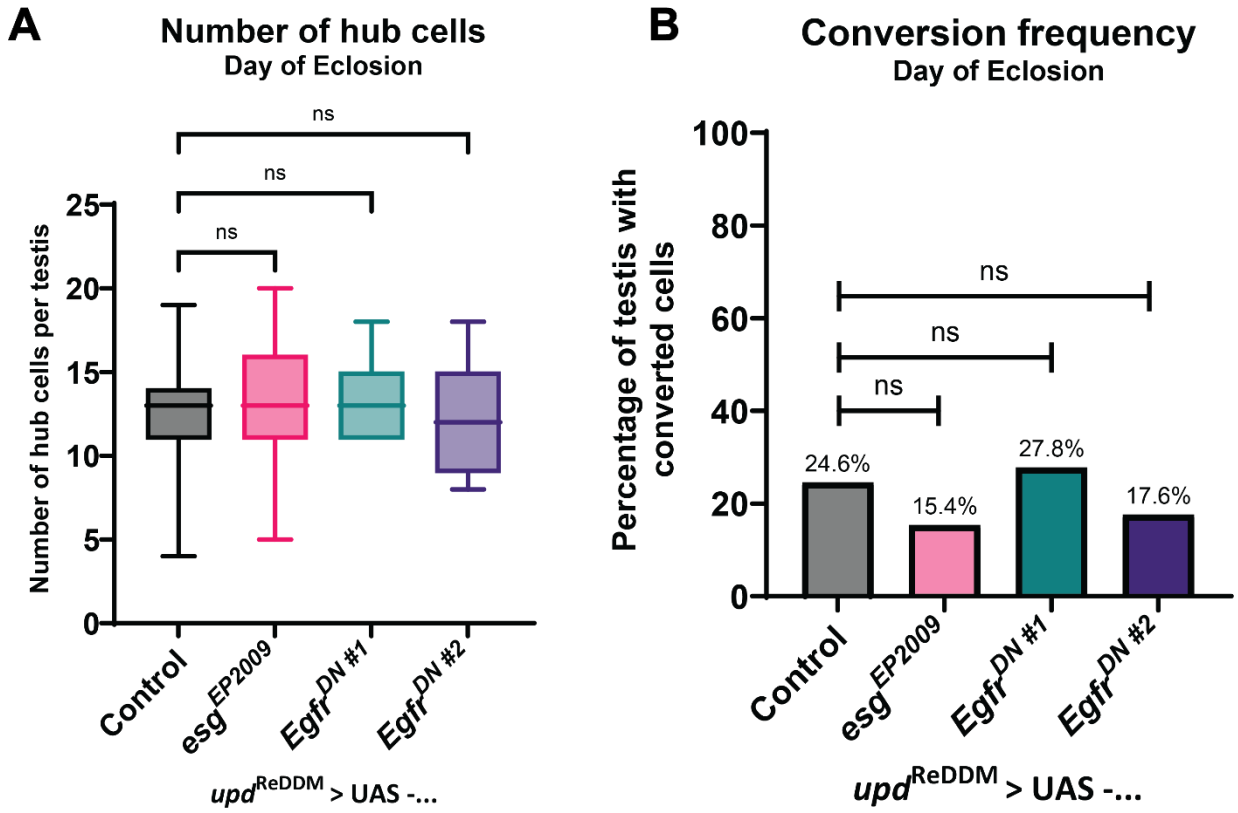

Figure 15: Manipulating *esg* and *Egfr* do not prevent hub remodeling. Transgenes esg^{EP2009} or $Egfr^{DN}$ were expressed with upd^{ReDDM} driver and lineage tracing tool between L3-Eclosion. (**A**) Number of hub cells (Fas3+) per condition. Statistical significance was determined by Kruskal-Wallis test. (**B**) Hub-to-CySC conversion frequency in adult testes on day of eclosion. Statistical significance was determined by Fisher's exact test.

Conclusion

In summary, the major findings of this project demonstrate that Escargot represses Egfr signaling under homeostatic conditions. When *esg* is depleted, MAPK activity increases (Figure 4). Ectopic activation of the Egfr-MAPK signaling machinery in hub cells induces hub-to-CySC conversion, much like *esg* depletion (Figure 7). Moreover, experiments utilizing Ras effector loop mutations point to Egfr-mediated conversion to be MAPK-dependent (Figure 8). Furthermore, we showed that repressing Egfr signaling suppresses hub-to-CySC conversion upon esg depletion (Figures 4 & 5). Conversely, overexpressing *esg* in CySCs increases early cyst cells and induces CySC-to-hub cell conversion, which importantly depends on Egfr since constitutive Egfr activation in CySCs prevents this conversion (Figures 10 & 11). Collectively, these findings support the hypothesis that Escargot acts upstream of Egfr to regulate somatic cell identity and maintain tissue homeostasis in the testis (Figure 16).

This project was not able to generate enough data to elucidate the mechanism by which Esg represses Egfr. The standing hypothesis is that Esg regulates *Egfr* transcriptionally, since Egfr was a significant hit in the Esg-DamID data set. Furthermore, according to our meta-analysis of the Fly Cell Atlas single-nucleus RNA sequencing dataset (Li et al., 2022), Egfr transcript levels are lower in CySCs than hub cells (Figure 17B), which is consistent the protein data presented in Figure 3B. Preliminary qPCR data from whole testes suggests that Egfr transcript increases upon *esg* depletion from hub cells (Figure 17A). However, when *esg* is depleted from hub cells in the presence of flies carrying the *Egfr::sfGFP* allele our *qualitative* analysis determined there was no noticeable difference in Egfr protein levels. There is an ongoing effort to develop an unbiased quantitative approach for addressing this hypothesis with the Egfr::sfGFP fusion protein.

Our lab has published multiple studies that have contributed to the current understanding of how Escargot influences cell fate in the fly intestine and testis. However, significantly less work has been done to uncover what might be upstream of Escargot. Previous studies were limited by the availability of tools and could only rely on mRNA or enhancer trap readouts. With the production of the Esg::mCherry fusion protein, we have a newfound ability to begin to interrogate which signals influence Esg levels. Having a functional fusion protein at our disposal unlocks previously unavailable assays and methods that will allow us to measure changes in Esg activity with increased resolution and nuance. For example, we can assess how Esg protein levels or localization changes in contexts where nonautonomous effects greatly impact hub biology, such as the expansion of the somatic cells in agametic testes, or hub-to-CySC conversion when CySCs are ablated. Additionally, the Esg::mCherry fusion line enables us to better assess if Esg levels fluctuate during normal physiological processes, as we observe with age. Since Esg has been shown to be such an important regulator of cell fate, understanding what is upstream of Esg may greatly elevate our understanding of how stem cell niches integrate multiple signals.

Our data unveiled a previously unrecognized model for Esg-mediated cell fate decisions in the *Drosophila* testis. It is a relatively small contribution when viewed in the context of the myriad of signaling networks coordinating with, or working against, each other to maintain homeostasis within the stem cell niche. While the findings may not be directly translatable to human disease today, we believe they will inform future experiments and aid in the collective scientific pursuit. We believe our results reiterate the strength of studying signal transduction in *Drosophila*, which remains a prolific research tool that continues to elevate our understanding of human development, disease, and regeneration.

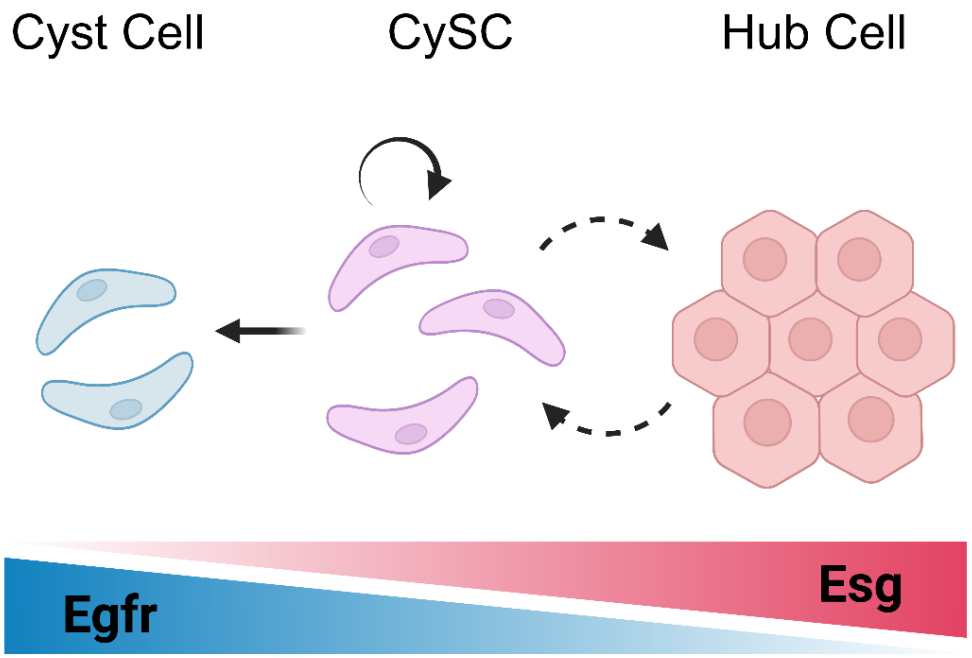

Figure 16: Model of Esg-Egfr relationship in directing somatic cell fate. A graphical abstract depicting the Esg-Egfr genetic relationship in controlling cell fate decisions at the testis apex. Diagram made with BioRender.

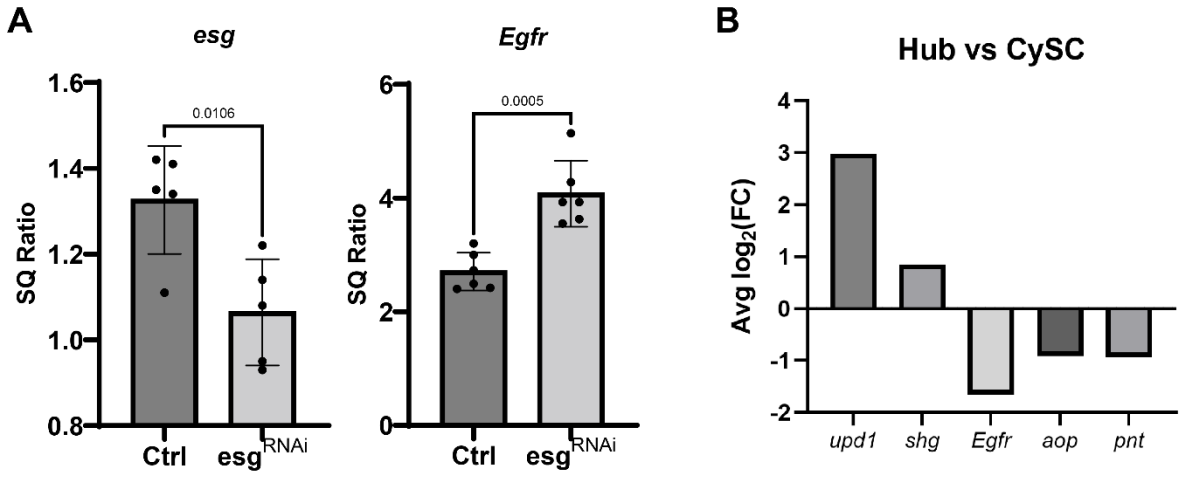

Figure 17: *Egfr* is transcriptionally regulated by Esg. (A) qPCR data from testes expressing upd^{TS}>*esg*$^{RNAi\ (GD)}$ for 3 days. mRNA of *esg* and *Egfr* were quantified. (B) Meta-analysis of testes

subset of Fly Cell Atlas single-nuclei RNA sequencing dataset depicting differentially expressed genes between hub cells and CySCs. Genes *upd1* and *shg* are biomarkers known to be enriched in hub cells. Genes *aop* and *pnt* are downstream nuclear effectors of the Egfr-MAPK signaling cascade.

Materials and Methods

Tissue-specific genetic manipulation

Transgene expression was restricted to adult tissue under cell-specific promoters in the presence of a temperature-sensitive GAL80. Crosses were performed and maintained at 18 °C for up to 5 days post eclosion. Transgene expression was induced through inactivating the GAL80 by shifting adult males to 29 °C. Flies maintained at 29 °C were transferred onto new food every 2-3 days until dissection. In experiments exploring the genetic interactions between two UAS-based constructs, the levels of UAS were consistently balanced with a reporter transgene (e.g., LacZ, GFP) to ensure a uniform availability of Gal4 across all experimental conditions. Transgenes were expressed in hub cells using updTS driver line (upd-Gal4; tub-Gal80TS;+). Transgenes were expressed CySCs and early cyst cells using c587TS (c587-Gal4;tub-Gal80TS;+) or tjTS (w; tj-Gal4; tub-Gal80TS).

Immunostaining

Testes from adult flies were dissected and fixed in a 4% paraformaldehyde solution for 30 minutes. Samples were washed twice in PBST (PBS, 0.1% Triton X-100) supplemented with 0.3% sodium deoxycholate for 5 minutes each, followed by two 10-minute washes in BSA buffer (PBS, 0.3% bovine serum albumin (BSA), 0.1% Triton X-100). Samples were incubated overnight at 4 °C with primary antibodies diluted in BSA buffer. Samples were subjected to three 10-minute washes in BSA buffer before secondary antibody incubation. Alexa-conjugated secondary antibodies (Invitrogen) were diluted in BSA buffer (1:250) and incubated with samples for 2 hours at room temperature, shielded from light. Samples received another three 10-minute washes in BSA buffer before being mounted onto microscope slides in VectaShield with DAPI (Vector Labs). Samples

were imaged with Carl Zeiss Axiovert 7 inverted microscopes equipped with either LSM 880 Airyscan, LSM 980 Airyscan 2, or Apotome 2 modules. Digital images were processed using ZEN Blue or ImageJ and organized into panels using Adobe Illustrator.

RNA Extraction and quantitative RT-PCR

Testes were dissected in cold PBS and flash frozen in liquid nitrogen in fresh TRIzol buffer (TRIzol, 5 µg Linear Poly-Acrylamide, 100 ng yeast tRNA) and stored at -80 °C. Frozen tissue was lysed by 5 rounds of freezing in liquid nitrogen (or dry ice) and thawing in a 37 °C heating block. To disrupt RNA-protein complexes, samples were vortexed on high 5 times in 30-second increments and rested for 5 minutes at room temperature. Total RNA was isolated by phenol/chloroform extraction (Cold Spring Harb Protoc; doi: 10.1101/pdb.prot101675) and quantified using a NanoDrop OneC spectrophotometer (Thermo Scientific).

Purified RNA (1 µg) was treated with RQ1 RNase-free DNase (Promega, M6101). DNnase-treated RNA was reverse-transcribed using the iScript supermix kit (Bio-Rad, 170-8841) with no protocol deviations. Standard qPCRs were carried out on a Bio-Rad CFX96 Touch System (Bio-Rad), using Sso Advanced SYBR Green (Bio-Rad, 1725-264). Cycling conditions were as follows: 95 °C for 30s; 95 °C for 5s, 52 °C for 30s (40 cycles); 65-95 °C, 0.5 °C increments at 2 sec/step. The following primer sequences were used (500 nM): Act5c (Fwd: TTGTCTGGGCAAGAGGATCAG; Rev: ACCACTCGCACTTGCACTTTC); esg (Fwd: CGCCAGACAATCAATCGTAAGC; Rev: TGTGTACGCGAAAAAGTAGTGG);

Generation of Escargot overexpression clones

Clones positively marked with GFP were generated using the MARCM technique (Lee and Luo, 1999). Two 2h-heat shock treatments at 37 °C were performed on the same day to induce the expression of the flippase enzyme and consequent FRT-mediated recombination.

Quantification and Statistical Analysis

Hub Cell Number Counts

To determine the number of hub cells per testis sample, IF was performed with antibodies against cohesion molecule Fasiclin 3 (Fas3). Z-Stack images were acquired using confocal-based microscopy with a 63x oil immersion objective on either an LSM 880 (0.24um Z-steps) or LSM 980 (0.15um Z-steps) equipped system. Z-dimension boundaries were gated on Fas3 immunosignal at the testis apex. Nuclei with at least 2 distinct cell borders positive for Fas3 were counted as hub cells. Raw counts were recorded in a GraphPad Prism matrix and plotted on a scatter plot. Nonparametric ANOVA analysis was performed in GraphPad Prism software on this matrix to determine the statistical significance of observed differences.

ReDDM Lineage Tracing

To determine the frequency of conversion events upon genetic manipulation, IF was performed with antibodies against GFP and/or DsRed on testis samples containing the UAS-H2B::RFP, tub-GAL80ts cassette. Cells positive for RFP but negative for GFP and other biomarkers were considered to be converted cells.

Hub-to-cyst cell conversion assayed using the updReDDM (upd-Gal4, UAS-GFP;; UAS-H2B::RFP, tub-Gal80TS) driver line was quantified by the number of testis samples that had at

least one RFP-positive, GFP-negative, Fas3-negative nuclei present at the tip of the testis. Background H2B::RFP signal is sometimes observed in late cyst cells or nuclei within the muscle sheath. Given their distinct location, these events were ignored and not included in the analysis. Data was recorded and compiled into a GraphPad Prism contingency table, transformed to be represented as fraction-of-total, and plotted as a contingency graph. Statistical significance was determined by conducting a two-sided Fisher's exact test on the raw data between each genetic manipulation and control sample (UAS-mCherryRNAi).

Cyst-to-hub cell conversion assayed using the c587ReDDM (c587-Gal4; UAS-GFP; UAS-H2B::RFP, tub-Gal80TS) driver line was quantified by counting the number of RFP-positive, Fas3-positive nuclei observed at the tip of the testis. Data was recorded and compiled into a GraphPad Prism contingency table, transformed to be represented as a fraction-of-total, and plotted on a contingency graph. Statistical significance was determined by conducting a two-sided Fisher's exact test on the raw data between each genetic manipulation and control sample (w1118 outcross).

MAPK Activity using Erk-nKTR reporter tool

To quantify changes in MAPK activity, Hub cell nuclei were manually segmented in FIJI and stored in the ROI-manager. Then, the average intensity of both Red and Green signals were measured per nuclei and reported as a ratio (Red/Green), as described in Yuen et al., 2022. Data was recorded and compiled in a GraphPad Prism matrix. Statistical significance was calculated with a nonparametric student t-test using GraphPad Prism Software with at least n=40 hub cells per condition. Error bars represent SEM.

Quantification of qPCR results

The Ct (cycle threshold) values were assayed via qPCR. The first ΔCt was calculated by subtracting the Ct value of the housekeeping gene (Act5c) from that of the gene of interest within each sample. Subsequently, the second ΔCt was computed by subtracting the average ΔCt of the control group from the ΔCt of the experimental group. This second ΔCt represented the change in gene expression relative to the control. The fold change in gene expression was then calculated using $2^{-\Delta\Delta Ct}$. This data was log-transformed to represent expression changes more intuitively. Statistical significance was determined by conducting a two-tailed unpaired t-test on the log-transformed data.

References

Amoyel, M., Anderson, J., Suisse, A., Glasner, J., & Bach, E. A. (2016). Socs36E Controls Niche Competition by Repressing MAPK Signaling in the Drosophila Testis. *PLoS Genetics*, *12*(1). https://doi.org/10.1371/journal.pgen.1005815

Antonello, Z. A., Reiff, T., Ballesta-Illan, E., & Dominguez, M. (2015). Robust intestinal homeostasis relies on cellular plasticity in enteroblasts mediated by miR-8-Escargot switch. *The EMBO Journal*, *34*(15), 2025–2041. https://doi.org/10.15252/EMBJ.201591517

Boyle, M., Wong, C., Rocha, M., & Jones, D. L. (2007). Decline in self-renewal factors contributes to aging of the stem cell niche in the Drosophila testis. *Cell Stem Cell*, *1*(4), 470–478. https://doi.org/10.1016/J.STEM.2007.08.002

DiNardo, S., Okegbe, T., Wingert, L., Freilich, S., & Terry, N. (2011). lines and bowl affect the specification of cyst stem cells and niche cells in the Drosophila testis. *Development (Cambridge, England)*, *138*(9), 1687–1696. https://doi.org/10.1242/DEV.057364

Greenspan, L. J., de Cuevas, M., Le, K. H., Viveiros, J. M., & Matunis, E. L. (2022). Activation of the EGFR/MAPK pathway drives transdifferentiation of quiescent niche cells to stem cells in the Drosophila testis niche. *ELife*, *11*. https://doi.org/10.7554/eLife.70810

Greenspan, L. J., & Matunis, E. L. (2018). Retinoblastoma Intrinsically Regulates Niche Cell Quiescence, Identity, and Niche Number in the Adult Drosophila Testis. *Cell Reports*, *24*(13), 3466-3476.e8. https://doi.org/10.1016/j.celrep.2018.08.083

Herrera, S. C., & Bach, E. A. (2018). JNK signaling triggers spermatogonial dedifferentiation during chronic stress to maintain the germline stem cell pool in the drosophila testis. *ELife*, *7*. https://doi.org/10.7554/ELIFE.36095

Herrera, S. C., Sainz de la Maza, D., Grmai, L., Margolis, S., Plessel, R., Burel, M., O'Connor, M., Amoyel, M., & Bach, E. A. (2021). Proliferative stem cells maintain quiescence of their niche by secreting the Activin inhibitor Follistatin. *Developmental Cell*, *56*(16), 2284-2294.e6. https://doi.org/10.1016/J.DEVCEL.2021.07.010

Hétié, P., de Cuevas, M., & Matunis, E. (2014). Conversion of Quiescent Niche Cells to Somatic Stem Cells Causes Ectopic Niche Formation in the Drosophila Testis. *Cell Reports*, *7*(3), 715–721. https://doi.org/10.1016/J.CELREP.2014.03.058

Hudson, A. G., Parrott, B. B., Qian, Y., & Schulz, C. (2013). A Temporal Signature of Epidermal Growth Factor Signaling Regulates the Differentiation of Germline Cells in Testes of Drosophila melanogaster. *PLOS ONE*, *8*(8), e70678. https://doi.org/10.1371/JOURNAL.PONE.0070678

Karim, F. D., & Rubin, G. M. (1998). Ectopic expression of activated Ras1 induces hyperplastic growth and increased cell death in Drosophila imaginal tissues. *Development (Cambridge, England)*, *125*(1), 1–9. http://www.ncbi.nlm.nih.gov/pubmed/9389658

Kiger, A. A., Jones, D. L., Schulz, C., Rogers, M. B., & Fuller, M. T. (2001). Stem cell self-renewal specified by JAK-STAT activation in response to a support cell cue. *Science (New York, N.Y.)*, *294*(5551), 2542–2545. https://doi.org/10.1126/science.1066707

Kiger, A. A., White-Cooper, H., & Fuller, M. T. (2000). Somatic support cells restrict germline stem cell self-renewal and promote differentiation. *Nature*, *407*(6805), 750–754. https://doi.org/10.1038/35037606

Kitadate, Y., & Kobayashi, S. (2010). Notch and Egfr signaling act antagonistically to regulate germ-line stem cell niche formation in Drosophila male embryonic gonads. *Proceedings of the National Academy of Sciences of the United States of America*, *107*(32), 14241–14246. https://doi.org/10.1073/pnas.1003462107

Korzelius, J., Naumann, S. K., Loza-Coll, M. A., Chan, J. S., Dutta, D., Oberheim, J., Gläßer, C., Southall, T. D., Brand, A. H., Jones, D. L., & Edgar, B. A. (2014). Escargot maintains stemness and suppresses differentiation in Drosophila intestinal stem cells. *The EMBO Journal*, *33*(24), 2967–2982. https://doi.org/10.15252/EMBJ.201489072

Li, H., Janssens, J., de Waegeneer, M., Kolluru, S. S., Davie, K., Gardeux, V., Saelens, W., David, F. P. A., Brbić, M., Spanier, K., Leskovec, J., McLaughlin, C. N., Xie, Q., Jones, R. C., Brueckner, K., Shim, J., Tattikota, S. G., Schnorrer, F., Rust, K., … Aerts, S. (2022). Fly Cell Atlas: A single-nucleus transcriptomic atlas of the adult fruit fly. *Science*, *375*(6584). DOI: 10.1126/science.abk243

Loza-Coll, M. A., Southall, T. D., Sandall, S. L., Brand, A. H., & Jones, D. L. (2014). Regulation of Drosophila intestinal stem cell maintenance and differentiation by the transcription factor Escargot. *The EMBO Journal*, *33*(24), 2983–2996. https://doi.org/10.15252/embj.201489050

Lu, Y., Yao, Y., & Li, Z. (2019). Ectopic Dpp signaling promotes stem cell competition through EGFR signaling in the Drosophila testis. *Scientific Reports*, *9*(1), 6118. https://doi.org/10.1038/s41598-019-42630-y

Miao, G., & Hayashi, S. (2016). Escargot controls the sequential specification of two tracheal tip cell types by suppressing FGF signaling in Drosophila. *Development (Cambridge, England)*, *143*(22), 4261–4271. https://doi.org/10.1242/dev.133322

Sênos Demarco, R., Stack, B. J., Tang, A. M., Voog, J., Sandall, S. L., Southall, T. D., Brand, A. H., & Jones, D. L. (2022). Escargot controls somatic stem cell maintenance through the

attenuation of the insulin receptor pathway in Drosophila. *Cell Reports*, *39*(3). https://doi.org/10.1016/j.celrep.2022.110679

Sênos Demarco, R., Uyemura, B. S., & Jones, D. L. (2020). EGFR Signaling Stimulates Autophagy to Regulate Stem Cell Maintenance and Lipid Homeostasis in the Drosophila Testis. *Cell Reports*, *30*(4), 1101-1116.e5. https://doi.org/10.1016/J.CELREP.2019.12.086

Tanaka-Matakatsu, M., Uemura, T., Oda, H., Takeichi, M., & Hayashi, S. (1996). *Cadherin-mediated cell adhesion and cell motility in Drosophila trachea regulated by the transcription factor Escargot*. *122*(12). http://dev.biologists.org/content/develop/122/12/3697.full.pdf

Voog, J., D'Alterio, C., & Jones, D. L. (2008). Multipotent somatic stem cells contribute to the stem cell niche in the Drosophila testis. *Nature*, *454*(7208), 1132–1136. https://doi.org/10.1038/nature07173

Voog, J., Sandall, S. L., Hime, G. R., Resende, L. P. F., Loza-Coll, M., Aslanian, A., Yates, J. R., Hunter, T., Fuller, M. T., & Jones, D. L. (2014). Escargot Restricts Niche Cell to Stem Cell Conversion in the Drosophila Testis. *Cell Reports*, *7*(3), 722–734. https://doi.org/10.1016/J.CELREP.2014.04.025

Wallenfang, M. R., Nayak, R., & DiNardo, S. (2006). Dynamics of the male germline stem cell population during aging of Drosophila melanogaster. *Aging Cell*, *5*(4), 297–304. https://doi.org/10.1111/J.1474-9726.2006.00221.X

Whiteley, M., Noguchi, P. D., Sensabaugh, S. M., Odenwald, W. F., & Kassis, J. A. (1992). The Drosophila gene escargot encodes a zinc finger motif found in snail-related genes. *Mechanisms of Development*, *36*(3), 117–127. https://doi.org/10.1016/0925-4773(92)90063-P

Yagi, Y., & Hayashi, S. (1997). Role of the Drosophila EGF receptor in determination of the dorsoventral domains of escargot expression during primary neurogenesis. *Genes to Cells*, *2*(1), 41–53. https://doi.org/10.1046/j.1365-2443.1997.d01-282.x

Yuen, A. C., Prasad, A. R., Fernandes, V. M., & Amoyel, M. (2022). A kinase translocation reporter reveals real-time dynamics of ERK activity in Drosophila. *Biology Open*, *11*(5). https://doi.org/10.1242/BIO.059364

Zhang, Q., Huang, H., Zhang, L., Wu, R., Chung, C. I., Zhang, S. Q., Torra, J., Schepis, A., Coughlin, S. R., Kornberg, T. B., & Shu, X. (2018). Visualizing Dynamics of Cell Signaling In Vivo with a Phase Separation-Based Kinase Reporter. *Molecular Cell*, *69*(2), 334-346.e4. https://doi.org/10.1016/J.MOLCEL.2017.12.008